Humidity Dependence of Bulk and Surface Resistivity of Polymers for HVDC Applications

DIEGO VALCARCE ALBA

DEPARTMENT OF ELECTRICAL ENGINEERING

CHALMERS UNIVERSITY OF TECHNOLOGY
Gothenburg, Sweden 2022
www.chalmers.se

Master's thesis 2022

Humidity Dependence of Bulk and Surface Resistivity of Polymers for HVDC Applications

DIEGO VALCARCE ALBA

CHALMERS
UNIVERSITY OF TECHNOLOGY

Department Electrical Engineering
Division of Electric Power Engineering
Chalmers University of Technology
Gothenburg, Sweden 2022

Humidity Dependence of Bulk and Surface Resistivity of Polymers for HVDC Applications
DIEGO VALCARCE ALBA

Supervisor: Adj. Prof. Olof Hjortstam, Hitachi Energy Research
Supervisor: Research Specialist Xiangdong Xu, Chalmers University of Technology
Examiner: Prof. Yuriy Serdyuk, Chalmers University of Technology

Master's Thesis 2022
Department of Electrical Engineering
Division of Electric Power Engineering
Chalmers University of Technology
SE-412 96 Gothenburg
Telephone +46 31 772 1000

Cover: Surface resistivity measuring setup.

Typeset in LaTeX
Printed by Chalmers Reproservice
Gothenburg, Sweden 2022

Humidity dependence of bulk and surface resistivity of polymers for HVDC applications

DIEGO VALCARCE ALBA
Division of Electric Power Engineering
Department of Electrical Engineering
Chalmers University of Technology

Abstract

Polymers are a key component of HVDC insulation systems. When insulation is exposed to a DC field, electrical charges tend to accumulate on polymeric surfaces that leads to modifications on the local electric field. Surface and bulk resistivities of polymers are fundamental material characteristics and their behavior under various operating conditions is crucial when it comes to predicting surface charging phenomena and designing an optimal and reliable insulation.
In the present work, dependencies of bulk and surface resistivities of three different silicon rubber materials used in HVDC applications on temperature and humidity of surrounding air were studied experimentally. The measurements were conducted using 1 mm thick samples installed in a three-electrode arrangement energised with the test voltage of 1 kV. The test setup was mounted inside a sealed oven, where the humidity was controlled using salt solutions. The measurements were performed at three levels of relative humidity (20-30%, 60% and 90%) and temperatures 30 °C and 60 °C.
The obtained results provided actual magnitudes of the measured characteristics, which are important for practical use of the polymer. It was found that both bulk and surface resistivities of all studied materials decrease with increasing temperature as well as air humidity. However, the character of these variations was distinctive for each material. Physical reasons for the observed effects are scrutinised. Furthermore, the sources of experimental errors and uncertainties in the measured data were analysed and improvements for the measurement procedure were suggested. Thus, it was noticed that at high humidity levels, water condensation caused formation of a water film bridging the gap between the measuring and guard electrodes in the tree-electrode system and methods to avoid this phenomenon were

explored. Also, it was noticed that a steady state of the measured current was not being fully reached even in four hour long experiments and longer measurement time has been recommended to obtain more accurate data.

Keywords: HVDC insulation, electric conductivity, electric resistivity, bulk resistivity, surface resistivity, silicone rubber, Teflon, humidity.

Acknowledgements

I would like to start by thanking my supervisors. Xiangdong, I have felt really comfortable working with you. Your practical mindset has really helped me move this project forward. Olof, thank you for your constant kind works of support, the help with the report and thank you for stretching the budget in order to provide some of the physical means required to carry out this project.Yuriy, thank you for your constant support, your openness and the fruitful discussions.
My gratitude also goes to Daniel Svensson and Avnish. Thank you for your company, your curiosity and the insightful discussions. Thank you for the help with the small things in the lab which are so important.
Daniel Ahlqvist, thank you for your good opposition.
Last but not least, gracias a mi familia for your support. I would not be here if it was not for you. Also thank you my friends in Gothemburg for being the light in the grey days.

Diego Valcarce Alba, Hisingen, June 2022

Contents

1

Introduction

This master thesis is part of a collaboration between Chalmers University and Hitachi Energy Research. In this chapter the background of the subject is presented, followed by the statement of the aim and the objectives. Next the scope is defined. Lastly, the structure of the report is described.

1.1 Background

The use of HVDC transmission lines is a well established and growing technology. For some applications it has proven to be more cost effective and have less losses than its AC counterpart, in certain cases actually being the only feasible option. Those applications are long-distance power transmission, submarine cables above 50 km or the connection of asynchronous networks [1].

For a reliable operation, a robust insulation system is needed. The particularities of DC electric field and the pursuit of higher and higher voltages in order to increase the power transfer capacity and reduce the losses pose challenges to the insulation design. With 3293 km, a transmission capacity of 12 GW and a rated voltage of 1100 kV the Changji-Guquan HVDC link in China, in operation since 2018, has the record in distance, transmission capactiy and voltage level [2].

A key component in insulation systems are polymers. They are used for example in bushings, string insulators or post insulators like the ones shown in Figure 1.1. In the presence of a DC electric field like the one depicted in Figure 1.2, charges will accumulate in the polymer-air interface resulting in local variations of the electric field. The way charges accumulate and the resulting field variations depend on the bulk and surface resistivities of the polymer. Bulk and surface resistivities are not constant parameters but depend on factors like

temperature, electric field or ambient humidity. Knowing the resistivities of different polymers for different ambient conditions is crucial to be able to design optimal and reliable HVDC insulation systems.

(a) Silicon rubber sheds.

(b) Post insulators consisting of load bearing insulator tubes made of epoxy resin and fiber-glass and housing made of silicon rubber.

Figure 1.1: Composite post insulators [3].

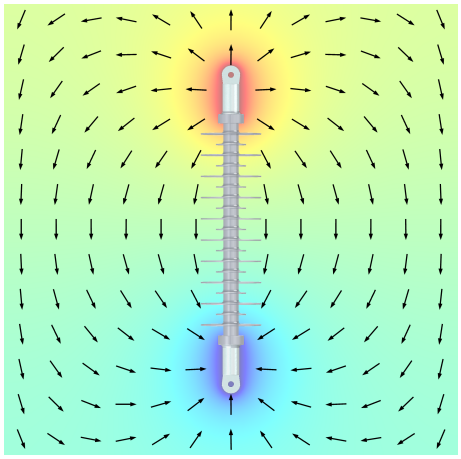

Figure 1.2: DC electric field in an insulator. From [4]. Reproduced with permission.

1.2 Aim

The aim of the work is to study the bulk and surface resistivities of several polymer materials (plate samples), under various humidities and temperatures. The polymers that will be studied are silicon rubber with various types of fillers and Teflon.

1.3 Objectives

In order to achieve the aim stated above, the following objectives are identified:

- Preparing the test setup. The different samples will be cut in the appropriate size an marked. During the measurements the samples will be set between electrodes that are connected to the resistivity measuring equipment. These electrodes will be ordered for manufacture and arranged properly. The necessary cables for the connection of the electrodes to the resistivity measuring equipment will be identified and adequate cable terminations will be prepared when necessary.
- Setting the temperature. A laboratory oven will be used to provide 30 and 60 °C ambient temperature. The oven will have to be insulated so that constant humidity conditions can be maintained.
- Setting the humidity. Salt solutions will be used to maintain various humidity levels (20%, 60% and 90%) [5]. The solutions will be prepared and the amount of solute will be calibrated.
- Determining the time the samples require to absorb the maximum amount of moisture. The samples will have to be exposed to the corresponding temperature and humidity conditions this amount of time before starting to measure the resistivity. The approximate time is known by Hitachi Energy researchers from experience. A method to confirm this which consists on measuring the loss factor evolution in a sample exposed to certain humidity and temperature conditions is explored.
- Measuring bulk resistivity.
- Measuring surface resistivity.
- Processing data. Scripts will be written in Matlab to process and plot the data from loss factor, humidity, temperature and resistivity measurements.
- Analysing the obtained results.

1.4 Scope

The materials that will be tested are the 1 mm thickness Teflon sample used in [4] and three 1 mm thickness silicon rubber samples purchased by Hitachi Energy Research from different manufactures. Materials are indicated in Table 1.1.

Table 1.1: Silicon rubber (SiR) and Teflon samples. PHR stands for parts per hundred resin, ATH stands for aluminum trihydrate and HTV stands for high temperature vulcanized.

Material/ Material alias	Curing agent	Filler
SiR/ Material 3	Peroxide	100 PHR silanized ATH
SiR/ Material 4	Peroxide	100 PHR silanized ATH
SiR/ Material 5	Pt catalyst	100 PHR silanized ATH
Teflon/ Teflon	N/A	N/A

The conditions under which each material's volume resistivity will be tested are indicated in Table 1.2. For each temperature and humidity conditions 3 measurements will be performed. For the lowest humidity condition at 60 °C the humidity will actually be 30% instead of 20%. The explanation is found in section 3.2.

Table 1.2: Test plan for volume resistivity. The number of measurements for each material under each temperature and humidity condition is indicated.

	Volume resistivity					
	20 % RH	30 % RH	60 % RH		90 % RH	
	30 °C	60 °C	30 °C	60 °C	30 °C	60 °C
Material 3	3	3	3	3	3	3
Material 4	3	3	3	3	3	3
Material 5	3	3	3	3	3	3
Teflon	3	-	-	-	3	-

The conditions under which each material's surface resistivity will be tested are indicated in Table 1.3. For each temperature and humidity conditions only one measurement will be performed. The lowest humidity will be 30% instead of 20%. The explanation is found in section 3.2. Material's 5 surface resistivity will not be measured because the size of the samples are too small for the electrode arrangement.

Table 1.3: Test plan for surface resistivity. The number of measurements for each material under each temperature and humidity condition is indicated.

	Surface resistivity					
	30 % RH		60 % RH		90 % RH	
	30 °C	60 °C	30 °C	60 °C	30 °C	60 °C
Material 3	1	1	1	1	1	1
Material 4	1	1	1	1	1	1
Material 5	-	-	-	-	-	-
Teflon	1	-	1	-	1	-

The exposure time of the samples to the temperature and humidity conditions will be 24 hours and the measuring time 4 hours.

1.5 Structure of the report

The report is structured as follows. Chapter 2 consists of the theory relevant for the project. In chapter 3 the methods are described. Results are presented and discussed in chapter 4. Conclusions are drawn in chapter 5. Finally suggestions for what to improve and future work are are presented in chapter 6.

2

Theory

2.1 Bulk and Surface resistivity

In this section the factors that influence DC bulk and surface resistivity in polymers are identified, the concepts of DC bulk and surface resistivity are derived and their measurement procedure is explained.

For simplicity DC resistivity will simply be referred to as resistivity.

Bulk and surface resistivities in polymers depend on multiple factors [6, 7, 8]. External factors are temperature, electric field, humidity, time, electrode arrangement. Internal factors are type of material, internal structure, impurities and fillers.

2.1.1 Bulk resistivity and how to measure it

Bulk or volume resistivity is determined by measuring the electric resistance of a material and taking into account its geometry.

The resistance is determined by applying a DC voltage to the material and measuring the resulting steady state current,

$$R = \frac{V}{I} \tag{2.1}$$

where R is the resistance, V is the DC voltage and I is the steady state DC current. The steady state DC current is further discussed in section 2.3. In the case the material is flat or a right prism, resistivity is given by

$$\rho = \frac{S}{L} \cdot R \tag{2.2}$$

where L is the dimension of the material in the direction of the electric field and S is the cross section of the material. The unit of bulk resistivity is the Ohm-metre (Ωm).

Figure 2.1 depicts a simplified section diagram of a three-electrode arrangement, used to measure bulk resistivity.

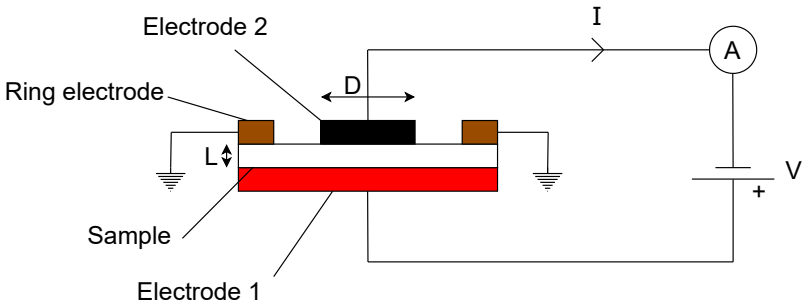

Figure 2.1: Three-electrode arrangement for bulk resistivity measurement.

It consists of 2 cylindrical electrodes (electrode 1 and 2), a ring electrode, a voltage source and an ammeter. Bulk resistivity can be calculated as

$$\rho = \frac{S}{L} \cdot R = \frac{\frac{1}{4}\pi D^2}{L} \cdot R \tag{2.3}$$

The objective of the ring electrode, which is grounded, is to stop the current that flows from electrode 1 over the surface of the sample from being measured. That way only the current that flows through the bulk of the sample is considered in the calculation of the resistivity. The ring electrode is called in this case the guard.

2.1.2 Surface resistivity and how to measure it

Surface resistivity is determined in a similar way to bulk resistivity. Surface resistance is obtained and then the geometry is taken into account. However, the calculation in this case is less straightforward. A derivation for the calculation of the surface resistivity is presented below. A more detailed explanation is found in [9].

Figure 2.2 depicts a simplified section diagram of a three electrode arrangement, used to measure surface resistivity.

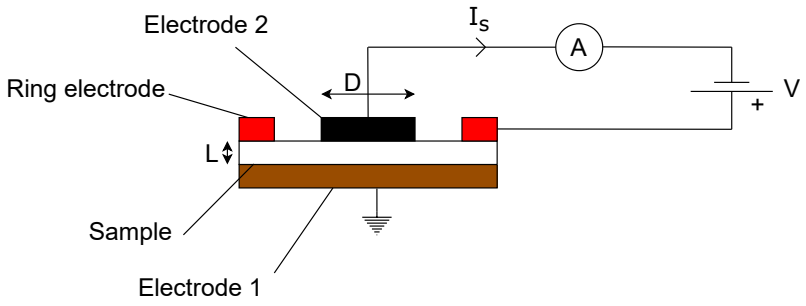

Figure 2.2: Three-electrode arrangement for surface resistivity measurement.

The ring electrode is the high voltage electrode. Current flows along the surface of the material sample from the ring electrode into electrode 2 and is measured. Grounding electrode 1 enables to take away the current that flows through the bulk of the material. Electrode 1 is in this case the guard.

Surface resistance is defined and calculated as

$$R_{\mathrm{S}} = \frac{V}{I_S} \tag{2.4}$$

where I_{S} is the steady state current that flows along the surface of the material sample from the ring electrode to electrode 2. The steady state DC current is further discussed in section 2.3. The unit of surface resistance is the same as of resistance, Ohm (Ω). In order to determine an expression for the surface resistivity, the differential form of Ohm's law for surface current density is used. Although it is a vector equation, only the module of its variables is considered:

$$j_S = \frac{E}{\rho_{\mathrm{s}}} \tag{2.5}$$

where ρ_{s} is the surface resistivity, E is the electric field magnitude at some point on the surface and j_{S} is the surface current density magnitude at that point. If an expression for j_{S} as a function of I_{S} and an expression for E as a function of the voltage, V, are found

then ρ_{s} as a function of the surface resistance and the geometry can be obtained.

Surface current density, j_{S}, is defined as the flux of charge through a differential length and its units are Ampere per metre (A/m). The current density at some point of the sample surface in the measurement arrangement of Figure 2.2 can thus be defined as

$$j_{\mathrm{S}} = \frac{I_S}{2\pi R} \tag{2.6}$$

where R is the radius of a circumference between the ring electrode and electrode 2 as can be seen in a top view of the three-electrode arrangement in Figure 2.3.

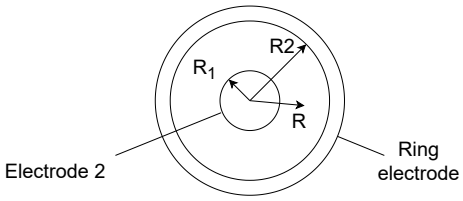

Figure 2.3: Top view three-electrode arrangement.

The voltage between the ring electrode and electrode 2 can be expressed as

$$V = \int_{R_1}^{R_2} E\mathrm{d}r \tag{2.7}$$

Substituting E for an expression derived from Equations 2.5 and 2.6,

$$V = \int_{R_1}^{R_2} \frac{\rho_{\mathrm{S}} I_{\mathrm{S}}}{2\pi r}\mathrm{d}r = \frac{\rho_{\mathrm{S}} I_{\mathrm{S}}}{2\pi}\ln\left(\frac{R_2}{R1}\right) \tag{2.8}$$

Rearranging,

$$\rho_{\mathrm{S}} = \frac{V \cdot 2\pi}{I_{\mathrm{S}} \cdot \ln\left(\frac{R_2}{R_1}\right)} \tag{2.9}$$

And finally substituting the surface resistance, the sought expression for surface resistivity is achieved:

$$\rho_S = \frac{R_S \cdot 2\pi}{\ln\left(\frac{R_2}{R_1}\right)} \tag{2.10}$$

Unlike resistivity, the unit of surface resistivity is the Ohm (Ω).

2.2 Polarisation

Understanding polarisation is key to understand the current response and the losses in a dielectric material. In this section a brief explanation of the phenomenon is given. Refer to [10] for a more detailed explanation.

Figure 2.4 shows the diagram of a dielectric material lying between 2 electrodes to which an external voltage V is applied.

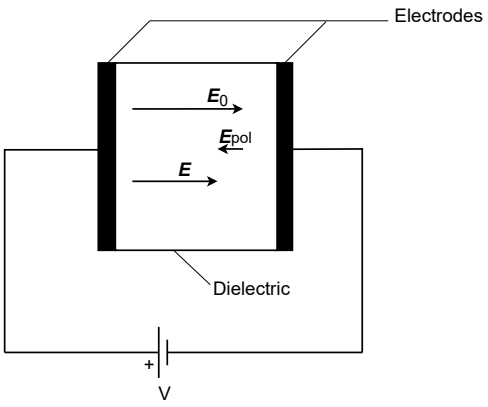

Figure 2.4: Polarisation in a dielectric.

The application of the external voltage V will lead to the flow of charges to the electrodes which will produce an electric field $\boldsymbol{E}$ in the dielectric. When the electrodes are parallel plates separated by a distance d much smaller than their size, $\boldsymbol{E}$ is approximately constant in the whole dielectric and given by

$$\boldsymbol{E} = \frac{V}{d}\hat{\boldsymbol{u}} \tag{2.11}$$

where $\hat{\boldsymbol{u}}$ is the unit vector perpendicular to the electrode plates pointing from high to low voltage. The presence of this field in the dielectric causes the displacement of charges and the aligning of charge dipoles

with the electric field. These cause an electric field $\boldsymbol{E}_{\text{pol}}$ to appear that opposes the external field. This phenomenon is known as polarisation.

$\boldsymbol{E}_0$, which is the electric field produced by the charges in the electrodes and is equal to $\boldsymbol{E}$ initially, before polarisation occurs, has to increase in order for the net field in the dielectric, $\boldsymbol{E}$, to remain constant. $\boldsymbol{E}$ remains constant because it is only determined by the externally applied voltage, V. The relation between $\boldsymbol{E}$, $\boldsymbol{E}_{\text{pol}}$ and $\boldsymbol{E}_0$ is given by

$$\boldsymbol{E} = \boldsymbol{E}_0 + \boldsymbol{E}_{\text{pol}} \tag{2.12}$$

Rearranging the equation,

$$\boldsymbol{E}_0 = \boldsymbol{E} - \boldsymbol{E}_{\text{pol}} \tag{2.13}$$

multiplying by the vacuum permittivity,

$$\epsilon_0 \boldsymbol{E}_0 = \epsilon_0 \boldsymbol{E} - \epsilon_0 \boldsymbol{E}_{\text{pol}} \tag{2.14}$$

and substituting $\epsilon_0 \boldsymbol{E}_0$ for $\boldsymbol{D}$ and $-\epsilon_0 \boldsymbol{E}_{\text{pol}}$ for $\boldsymbol{P}$,

$$\boldsymbol{D} = \epsilon_0 \boldsymbol{E} + \boldsymbol{P} \tag{2.15}$$

where $\boldsymbol{D}$ is the displacement field which is only determined by the charges in the electrodes independently of the dielectric material and has the unit Coulomb per square metre (C/m^2) and $\boldsymbol{P}$ is the polarisation which also has the unit Coulomb per square metre (C/m^2).

2.2.1 Polarisation mechanisms

It has been briefly mentioned that polarisation is caused by the displacement of charges and orientation of dipoles in a dielectric material subjected to an electric field. Polarisation mechanisms can be more thoroughly classified in [10]:

- Deformation polarisation. It is the displacement of electrodes with respect to the nuclei of atoms or the displacement of parts of molecules with different charges.
- Lattice polarisation. It is the displacement of lattice elements with different charges.

- Orientation polarisation. It is the orientation of polar molecules (dipoles) in the electric field direction.
- Interfacial polarisation. It is the accumulation of charges in interfaces of materials with different conductivities.

2.2.2 Polarisation losses

The displacement of charges and the orientation of dipoles lead to particle collisions which cause energy dissipation. When the frequency of the applied voltage is too low the power losses are low because there are little collisions per unit time. When the frequency of the applied voltage is too high, due to particle's inertia there is barely any polarisation and thus power losses are also low. Each polarisation mechanism has a frequency at which power losses are maximised.

2.3 Current Response of a Dielectric

A dielectric material can be represented by an equivalent circuit like the one shown in Figure 2.5. It enables to model the current response of the material to a DC voltage step which can be divided in 3 parts in the time domain.

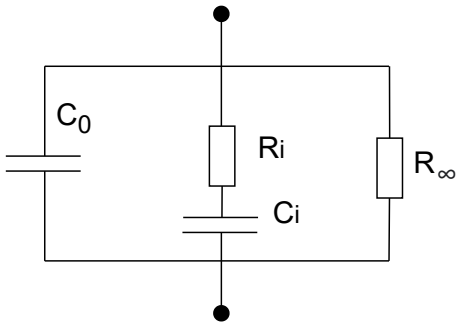

Figure 2.5: Dielectric material model.

The first part is the capacitive current which is the current surge that is measured just after a DC voltage step is applied. It is the current that charges the electrodes until the voltage between them equals the applied voltage and a field $\boldsymbol{E}$ appears in the dielectric. In the equivalent circuit it is the current that flows into C_0.

The second part is the polarisation current. The electric field in the dielectric, $\boldsymbol{E}$, causes its polarisation, given by $\boldsymbol{P}$. $\boldsymbol{E}$ remains constant because it is given by the externally applied voltage as shown in Equation 2.11. Therefore, the appearance and increase in $\boldsymbol{P}$ causes a increase in $\boldsymbol{D}$ as shown in Equation 2.15. As a result there is an additional flow of charges to the electrodes. Polarisation current is modeled by the $R_\mathrm{i}C_\mathrm{i}$ branch in the equivalent circuit. Each polarisation mechanism should be modeled by its own $R_\mathrm{i}C_\mathrm{i}$ branch but it is enough to consider one to set the general picture. Polarisation occurs fast initially and slows down as it approaches steady state. This translates into a current that reduces exponentially. Figure 2.6 shows the typical shape of the polarisation current and the conduction current in steady state which is discussed next.

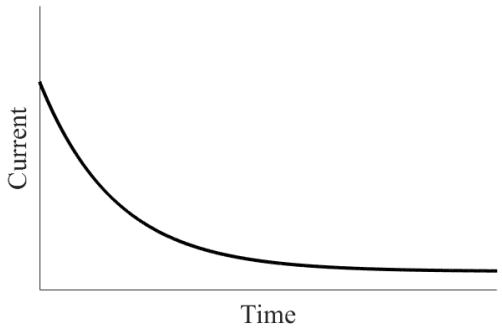

Figure 2.6: Current response of a dielectric to a DC voltage step

The third part is the leakage or conduction current. It is the DC current that flows through the dielectric material and is modeled by the current flowing through R_∞ in Figure 2.5. Although a differentiation between 3 different currents has been made, the conduction current is present since the initial instant of the current response. Its low value however makes it negligible initially.

2.4 Loss factor

If a sinusoidal AC voltage ($\underline{V}$ in phasor representation) is applied to the terminals of a capacitor and more generally to the terminals of 2 electrodes separated by a dielectric material the resulting current phasor, $\underline{I}$, is expected to lead $\underline{V}$ by an angle φ of 90^o. However, in practice, φ is not exactly 90^o but slightly smaller because of the losses

in the dielectric. As shown in Figure 2.7 the angle between $\underline{I}$ and the normal to $\underline{V}$ is the angle δ.

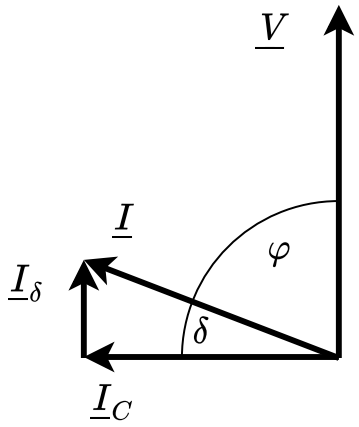

Figure 2.7: Voltage and currents in the complex plane for two electrodes separated by a dielectric.

The losses in the dielectric are related to δ. However it is more convenient to use $\tan(\delta)$ instead, which is called the loss factor.

As indicated in Figure 2.7 the current phasor can be split in a component parallel to the voltage, $\underline{I}_\delta$, which is related to the active power losses, and a component perpendicular to the voltage, $\underline{I}_C$, which is related to the reactive power. The loss factor can thus be expressed as

$$tan(\delta) = \frac{I_\delta}{I_\mathrm{C}} \tag{2.16}$$

Multiplying numerator and denominator by the module of the voltage,

$$\tan(\delta) = \frac{I_\delta V}{I_\mathrm{C} V} = \frac{P_\delta}{Q} \tag{2.17}$$

where P_δ are the active power losses and Q is the reactive power. Equation 2.17 establishes the relationship between the active power losses and angle δ.

The way $\tan(\delta)$ is typically measured is as a function of the applied voltage frequency. As can be seen in Figure 2.8 for lower frequencies $\tan(\delta)$ increases and tends asymptotically to infinite. This can

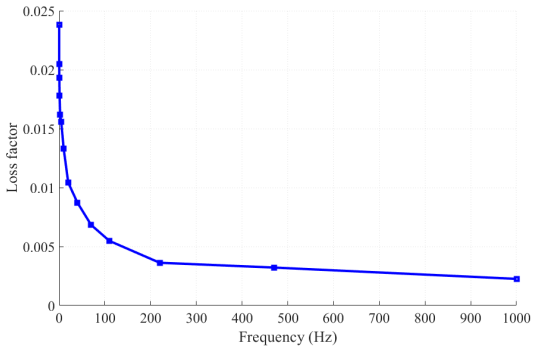

Figure 2.8: Example of loss factor in the frequency domain.

be understood knowing that Q will approach zero as the frequency approaches zero.

The losses in the dielectric material can be classified as conduction losses and polarisation losses. The higher the water content of the dielectric the higher the conduction losses (conductivity increases) and the higher the polarisation losses (water is a polar molecule) [10].

2.5 Humidity and humidity control

Humidity refers to the amount of water vapor in air. Two main ways of expressing humidity are absolute humidity and relative humidity. Absolute humidity is the mass of water vapor per unit volume of air.

$$AH = \frac{m_{\mathrm{v}}}{V_{\mathrm{air}}} \tag{2.18}$$

where AH is the absolute humidity, m_{v} is the mass of water vapor and V_{air} is the air volume.

Relative humidity expresses the amount of water vapor in air with respect to the amount of water vapor in saturation. Saturated air is air that contains the maximum amount of water vapor before condensation occurs and a liquid water phase appears. Therefore, relative humidity is the amount of water vapor in air relative to the maximum amount of water vapor that can be in an air volume. Relative humidity can be expressed as

$$RH = \frac{m_{\mathrm{v}}}{m_{\mathrm{g}}} \tag{2.19}$$

where RH is the relative humidity, m_{v} is the mass of water vapor and m_{g} is the mass of water vapor in saturated air which is a function of temperature. Relative humidity thus depends on temperature. The higher the temperature the higher m_{g}.

Both water vapor and dry air (air with no water vapor) can be described as ideal gases. They behave as if they existed alone in a certain volume and they follow the ideal gas relation $PV = nRT$ [11]. Therefore relative humidity can also be expressed as

$$RH = \frac{P_{\mathrm{v}}V/RT}{P_{\mathrm{g}}V/RT} = \frac{P_{\mathrm{v}}}{P_{\mathrm{g}}} \tag{2.20}$$

where P_{v} is the partial pressure of water vapor, R is the ideal gas constant, T is the temperature and P_{g} is the partial pressure of water vapor in saturation or simply saturation vapor pressure. This formulation is convenient because P_{g} is a well known and tabulated function of temperature. Relative humidity is typically expressed in percentage,

$$RH\% = \frac{P_{\mathrm{v}}}{P_{\mathrm{g}}} \cdot 100 \tag{2.21}$$

2.5.1 Humidity control

Having a closed chamber filled with air, if a open water container is introduced in it, water will evaporate until saturation is reached (if there is enough water in the container). Namely, relative humidity will reach 100 % in the closed volume.

Equilibrium can be displaced if instead of pure water, the container is filled with a salt solution as explained in [4]. The equilibrium humidity level will be lower. The higher the concentration of the solution the lower the equilibrium humidity.

Then it can be said that humidity in a closed volume of air can be controlled using a salt solution whose concentration is controlled. A particularly convenient way of doing this is by using saturated salt solutions. That is, solutions where the amount of solute is so high that a solid phase appears. Controlling the concentration of a solution is not easy task, specially given that water needs to evaporate before equilibrium is reached. In a saturated salt solution even if water evaporates

the concentration remains constant. The drawback is that a certain salt can only provide one equilibrium relative humidity. That is why different salt solutions have to be used in order to achieve different humidity levels.

Different saturated salt solutions lead to different relative humidities in equilibrium. These values are approximately constant in certain temperature ranges. A list of salts and the relative humidities that can be achieved with them can be found in [5].

3

Methods

3.1 Sample handling

Samples, as shown in Figure 3.1, are cut in the appropriate shape and size and marked. The number of holes in the sample indicates the material number according to Table 1.1. Teflon is not marked since there is only one sample of it.

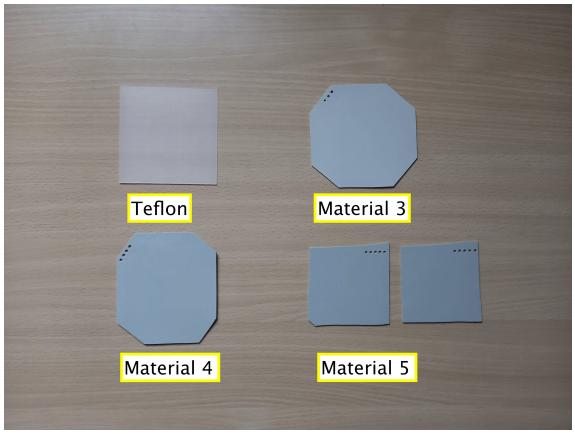

Figure 3.1: Material samples. Silicon rubber samples are grey although they seem blueish in this image.

When the polymeric samples are exposed to certain humidity conditions they absorb water from the ambient until an equilibrium is reached. The higher the ambient humidity the more water absorbed by the sample. Removing the water content from the sample is harder. It takes longer for a sample to dry and reach a new equilibrium when exposed to lower humidity conditions. The absolute humidity in the case of 30 °C, 20% relative humidity will sometimes be below the absolute humidity in the laboratory. Additionally, performing measurements at incremental absolute humidities is not desired to be the dominant factor in the planning of the measurements. Therefore, in order to accelerate the drying of the samples before exposing them to

lower humidity conditions, they are stored in a sealed vessel with silica gel as shown in Figure 3.2. The silica gel absorbs water and provides the very low relative humidity of 10 % inside the vessel.

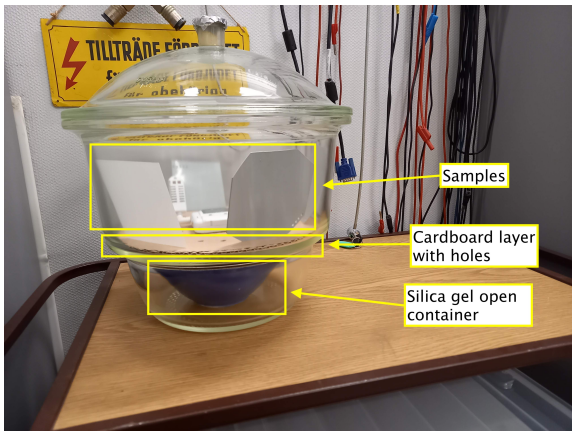

Figure 3.2: Sample dryer.

3.2 Temperature and humidity conditions

In order to control temperature, measurements are run inside the laboratory oven Memmert UN55 shown in Figure 3.3. This oven is not prepared to control humidity, that is why all air entry points are sealed using aluminium tape.

Figure 3.3: Laboratory oven Memmert UN55.

Humidity is measured with the sensor Thermo Recorder TR-73U from TandD shown in Figure 3.4a and the sensor EL-USB-2 from Lascar Electronics shown in Figure 3.4b.

(a) Humidity sensor for low temperature.

(b) Humidity sensor.

Figure 3.4

Humidity is controlled using salt solutions as explained in section 2.5.1. The salt solutions are kept in open containers at the bottom part of the oven as is shown in Figure 3.5. The salt solutions used to obtain each humidity level are indicated in Table 3.1.

Figure 3.5: Bulk resistivity measurement arrangement.

Table 3.1: Salt solutions used to achieve each humidity level.

	20% - 30%	60%	90%
30 °C 60 °C	Potasium acetate (saturated)	Magnesium chloride (unsaturated)	Potasium nitrate (saturated)

The steady state measured humidity levels lie within the indicated values plus minus 5%. The reason why for the lowest humidity level 20%-30% is indicated instead of simply 20% is that for different temperatures and at different times, different stable humidity values have been obtained.

When a saturated potassium acetate solution was exposed to 30 °C, an stable 20% relative humidity value was reached as shown in Figure 3.6.

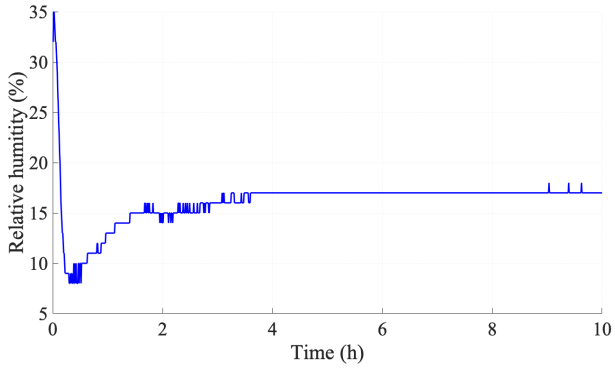

Figure 3.6: 20% relative humidity, 30 °C.

When the temperature is increased to 60 °C, unlike with the other salt solutions used, the relative humidity goes up to 30% as shown in Figure 3.7.

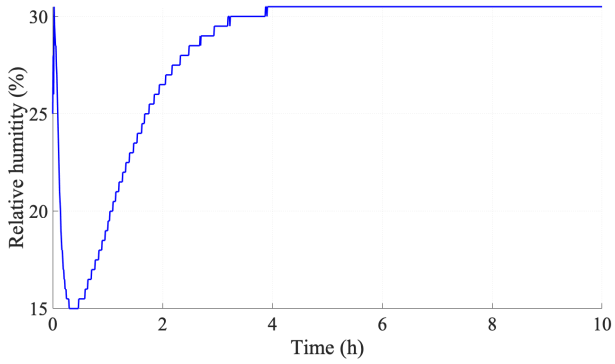

Figure 3.7: 30% relative humidity, 60 °C.

Bulk resistivity measurements were performed in the winter months, when the laboratory absolute humidity was below the absolute humidity at 30 °C, 20% relative humidity. However, surface resistivity measurements were performed in the spring months, when the laboratory absolute humidity was above the absolute humidity at 30 °C, 20% relative humidity. This resulted in the fact that relative humidity had to go down in the oven when setting a 20% relative humidity by using a saturated potasium acetate solution. It turned out the time to steady state then was much longer than when humidity had to go up. Measurements were performed at a relative humidity value of 30% that can be considered stable as shown in Figure 3.8. This is of course an intermediate step before relative humidity would reach 20% relative humidity in steady state.

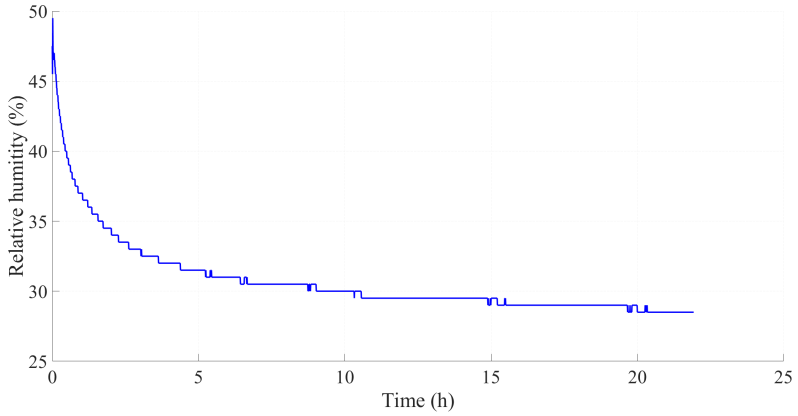

Figure 3.8: Relative humidity for the measurement of surface resistivity at 30 °C and the lowest humidity level.

The time it took for the humidity conditions in the oven to reach 95% of the intended final value is indicated in Table 3.2. Taking these values as reference it was decided that **8 hours** would be the time before exposure time of the samples would start to count. The exposure time is the time the samples have to be exposed to a certain temperature and humidity condition before performing the resistivity measurements and it was decided to be **24 hours**. This is a conservative choice that has been confirmed as enough after running an experiment that consisted in the measurement of the evolution of the loss factor as explained in section 3.4. The total time the samples were in the oven with the salt solutions is $8 + 24 = \mathbf{32\ hours}$, before the measurements started. Figure 3.9 shows this in a diagram.

Table 3.2: Observed 95% of the time to steady state in each salt solution.

	20%	60%	90%
30 °C	3 hours	3 hours	2.5 hours
60 °C	3 hours	5 hours	6 hours

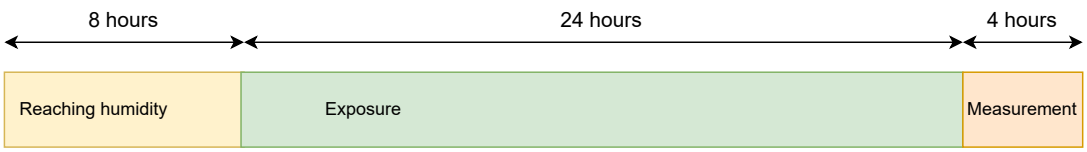

Figure 3.9: Experiment sequence.

Salt solutions are a cheap method to obtain a steady state humidity level in a closed chamber, however, some inconveniences have been encountered. The achieved steady state humidity values have not always exactly matched. If the oven is opened it instantly acquires the laboratory humidity conditions and it takes about half the time indicated in Table 3.2 to go back to steady state.

3.3 Bulk and surface resistivity measurement

Bulk and surface resistivity are determined by measuring the electric resistance of a material and taking into account its geometry as explained in section 2.1.

The electrometer 6517B from Keithley shown in Figure 3.10 is used to apply a voltage of **1 kV** and measure the current which is in the nano and pico range. The device is interfaced by a LabVIEW program that also enables to retrieve the data.

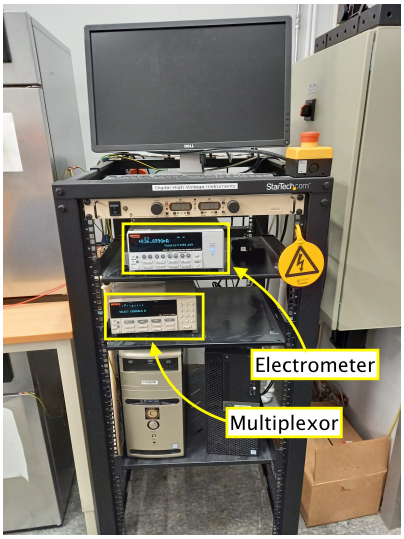

Figure 3.10: Electrometer and multiplexor.

The initial current measured by the electrometer cannot be used to determine the resistivity because it contains capacitive and polarisation components as explained in section 2.3. The current flowing through the dielectric is expected to reduce exponentially until it is purely conduction current in steady state. The time it would take to reach something that can be called steady state with the samples tested in the present project would be too long, that is why a compromise was made and **4 hours** was chosen to be the measuring time

as indicated in Figure 3.9. The resistivity values provided in chapter 4 are the average during the last hour of measurements. In the case of bulk resistivity measurements, where 3 measurements are taken for each material and ambient condition, it is also the average of the 3 different measurements.

3.3.1 Bulk resistivity measurement

Continuing with the notation from Figure 2.1 the brass electrodes used are shown in Figures 3.11 and 3.12. The gap distance between electrode 2 and the guard is in the order of tenths of a millimeter. Polyamide tape is used to maintain the gap distance.

(a) (b)

Figure 3.11: Bulk resistivity top electrodes.

Figure 3.12: Electrode 1 or bottom electrode.

In order to accelerate the testing phase, a multiplexor (see Figure 3.10) is used in order to be able to perform 6 measurements a the same time. The multiplexor continuously changes the selection of the analogue signal that is being measured at the electrometer. Three measurements are performed in each sample simultaneously and 2 samples are

measured in parallel. This requires 2 bottom electrodes and 6 top electrodes. The whole arrangement can be seen in Figure 3.13. Due to the small size of material 5 samples, an additional bottom electrode is present to be able to split the three top electrodes between the two samples. Connections are done as per Figure 2.1. The bottom electrodes are connected to the high voltage side of the electrometer through a HV cable. The top electrodes are connected to the electrometer through coaxial cables. The inner part of the cable is connected to electrodes 2 and the outer part of the cable is connected to the guards. The outer part of the cable is at ground potential.

Figure 3.13: Bulk resistivity measurement arrangement.

During exposure time the top electrodes are not positioned on the samples so that the material can be in full contact with the ambient conditions. Just before the measurement the door of the oven is opened and the top electrodes are put in place and connected. This, however, causes the humidity conditions in the oven to become equal with the laboratory ones and the desired values are not recovered at least until half the time indicated in Table 3.2 has passed. This means bulk resistivity measurements are conducted at an ambient condition different from the one intended. Nevertheless, it should not affect the results much since the critical thing in bulk resistivity is the exposure of the samples to the humidity conditions before measuring, so that the material absorbs all the water it has to.

3.3.2 High humidity bulk resistivity measurement

In high humidity conditions like 90% relative humidity, condensation is observed on the walls of the oven. It is not observable on the

sample but it may still occur in a microscopic scale as the results from section 4.2.1 suggest. Condensation may be leading to the bridging of electrode 2 and the guard or even the bridging of electrode 1 and electrode 2.

Apart from the conventional method explained in the previous section, two other procedures are explored. One consists of adding Teflon tape to the top of the top electrodes aiming to impede condensed water to penetrate the gap between electrode 2 and the guard (Figure 3.14a). The other one consists on removing the guards as shown in Figure 3.14b.

(a) Top electrode with Teflon tape.

(b) Bulk resistivity measurement arrangement without guards.

Figure 3.14: Alternative methods for measuring bulk resistivity at high humidities.

3.3.3 Surface resistivity measurement

The brass electrodes used are the same than in the case of bulk resistivity measurements except for the ring electrode, which is now the one shown in Figure 3.15.

The multiplexor described in section 3.3.1 is again used for surface resistivity measurements. In this case 3 measurements are performed simultaneously so that the surface resistivity of 3 samples can be measured in parallel. The whole arrangement can be seen in Figure 3.16. Connections are done as per Figure 2.2. Electrodes 1 are grounded by placing them on the oven tray which is itself grounded. They are the guard electrodes. The ring electrodes are connected to the high

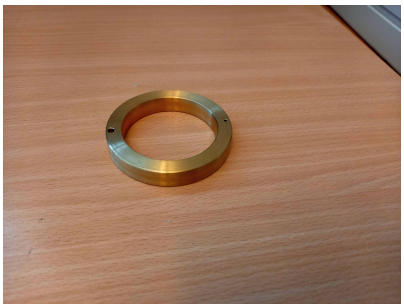

Figure 3.15: Ring electrode surface resistivity measurement.

voltage side of the electrometer via a HV cable. Electrodes 2 are connected to the electrometer through coaxial cables. The outer part of cable is grounded using crocodile clips.

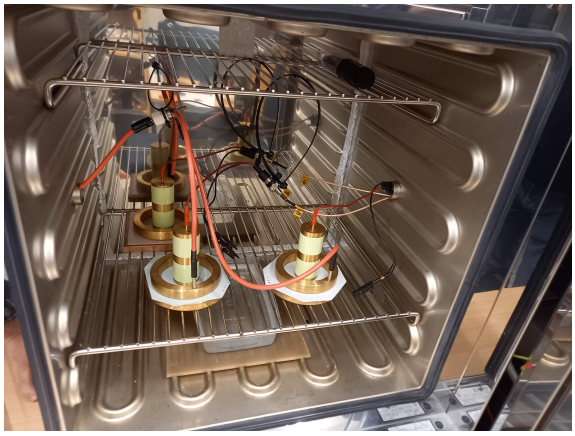

Figure 3.16: Surface resistivity measurement arrangement.

In order for the resistivity calculation to be correct, electrode 2 has to be concentric with the ring electrode, otherwise the current would not distribute uniformly. This is achieved by using the 3D printed piece produced for this purpose that is shown in Figure 3.17.

(a)

(b)

Figure 3.17: Positioning of electrode 2 and the ring electrode for surface resistivity measurement.

Unlike the case of bulk resistivity measurements, in the case of surface resistivity, the electrodes can be positioned during exposure because the relevant part of the sample is in full contact with ambient conditions. Thereby, the door of the oven does not have to be opened before the measurements and the right humidity conditions are present during the measurements.

3.4 Loss factor measurement

According to the experience in Hitachi Energy Research with polymer resistivity measurements at different humidities, it is known that approximately 6 hours is enough exposure time for a 1 mm silicon rubber sample with ATH filler to reach close to its maximum amount of water content and approximately 24 hours are needed to fully reach the maximum. In this project it is decided to expose the samples to the controlled ambient conditions for 24 hours before performing the measurements. In order to confirm the adequacy of this choice the experiment described below is conducted.

A silicon rubber sample is exposed to 30º and 90 % relative humidity. One of the 1 mm thickness samples whose resistivity will be measured is chosen. It is expected that different silicon rubber samples have similar minimum exposure time. The ambient condition of 30º and 90 % relative humidity is chosen because is one of the ambient conditions that has the highest absolute humidity and thus a higher minimum exposure time is expected.

An AC voltage is initially applied to the sample and the loss factor is measured. Then, successive loss factor measurements are taken for a 26 hour period. It is expected that as the humidity content of the sample increases, the loss factor increases. If the loss factor value reaches steady state within 24 hours the choice of this exposure time is adequate.

3.4.1 Electrode arrangement

The sample is put in between 2 electrodes, a HV electrode on top (Figure 3.18a) and a measuring electrode cast together with a guard electrode at the bottom (Figure 3.18b).

(a) High voltage electrode.

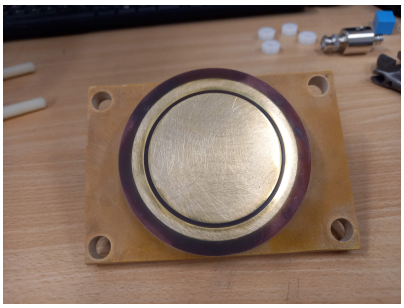

(b) Measuring electrode cast together with grounded ring electrode.

Figure 3.18: Electrodes used in the loss factor measurement.

As seen in Figure 3.19a the electrode arrangement is put together using an structure made of insulating material. As seen in Figure 3.19b a gap between the sample and the top electrode is left so that at least one of the surfaces of the sample can be constantly exposed to the controlled humidity. The gap length is 0.85 mm. This is achieved by putting the 1 mm silicon rubber sample between two layers of plastic that together have the desired gap length. This three layer piece is put between the electrodes which are then pressed together. The three layer piece is removed thanks to the lack of stickiness of the plastic. As a result the space between electrodes has now the right length to accommodate a 1 mm silicon rubber and leave a 0.85 mm gap.

(a) Electrode arrangement for loss factor measurement without silicon rubber sample.

(b) Electrode arrangement for loss factor measurement with silicon rubber sample.

Figure 3.19: Electrode arrangement for loss factor measurement.

The way the electrodes are connected to the device that generates the

AC voltage and measures the loss factor is indicated in Figure 3.20.

The high voltage side of the measuring devise is connected to a coaxial cable. The inner part of the coaxial cable, which carries the high voltage is connected through a banana connector to the upper electrode and the outer part of the coaxial cable, which is at ground potential is connected through a crocodile clip connector to the body of the oven which is grounded. This can be seen in the left part of Figure 3.20a.

The low voltage side of the measuring device is connected to a coaxial cable. The inner part of the cable is connected to the measuring electrode and the outer part of the cable is connected to the ring electrode which is grounded. This can be seen in the right part of Figure 3.20a. Grounding the ring electrode enables to take away the current that flows along the surface of the sample from the measurement.

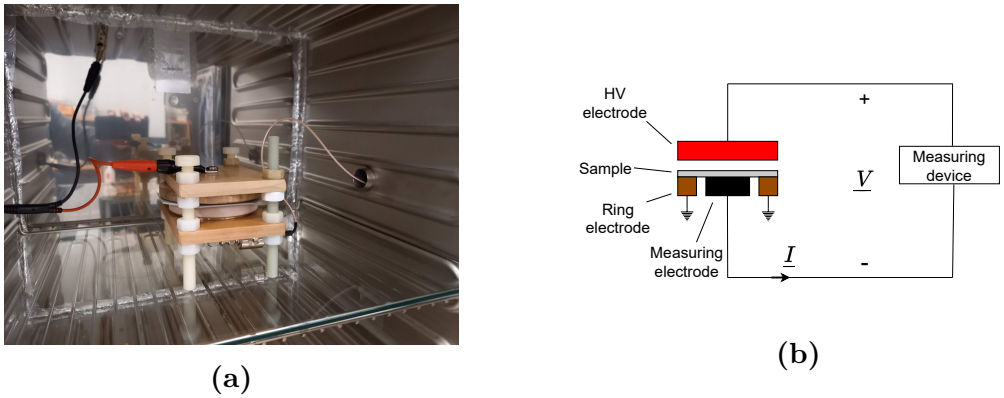

(a) (b)

Figure 3.20: Electrode arrangement for loss factor measurement connection.

3.4.2 Measuring device

The measuring device is a Megger IDAX 300 which is shown Figure 3.21. It enables to perform dielectric spectroscopy measurements, that is, measuring dielectric properties (capacitance, loss factor, ...) of a material as a function of frequency.

The Megger IDAX 300 applies a sinusoidal voltage, in this case a 140 Vrms voltage is chosen, and the response current is measured. The impedance is calculated and from this value different parameters like the capacitance or the loss factor can be calculated. The frequency of the voltage is varied, in this case the chosen frequency range is 0.1 to 1000 Hz.

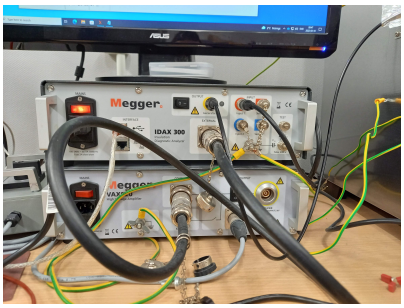

Figure 3.21: Megger IDAX 300.

4

Results and Discussion

4.1 Loss factor results and discussion

The results of measuring the loss factor in the frequency domain at different instants over a 26 hour period are shown in Figure 4.1. As expected the loss factor increases as the time the sample is exposed to 30º and 90 % humidity increases.

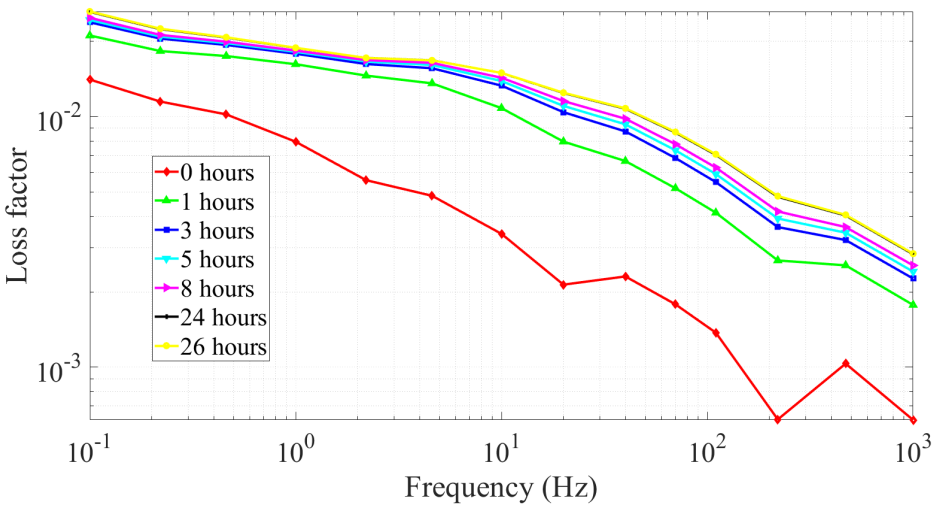

Figure 4.1: Loss factor measurements over 26 hours.

The difference between the measurement taken after 8 hours and the measurement taken after 24 hours is still noticeable. The relative difference between the two measurements in percentage is plotted and shown in Figure 4.2.

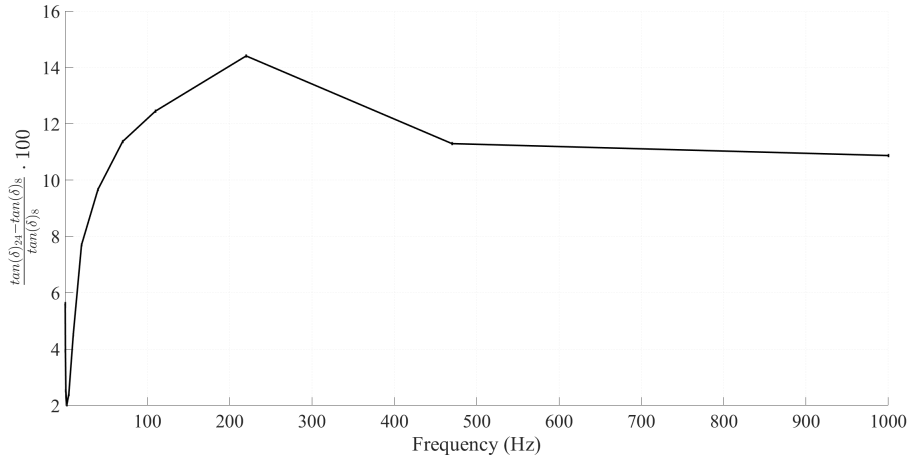

Figure 4.2: Relative difference between the loss factor measurement after 8 and 24 hours in percentage.

The measurement taken after 26 hours overlaps with the measurement taken after 24 hours. This would indicate that after 24 hours a sufficient steady state is reached. The relative difference between the two measurements in percentage is plotted and shown in Figure 4.3. The small values confirm that a sufficient steady state has been reached after 24 hours.

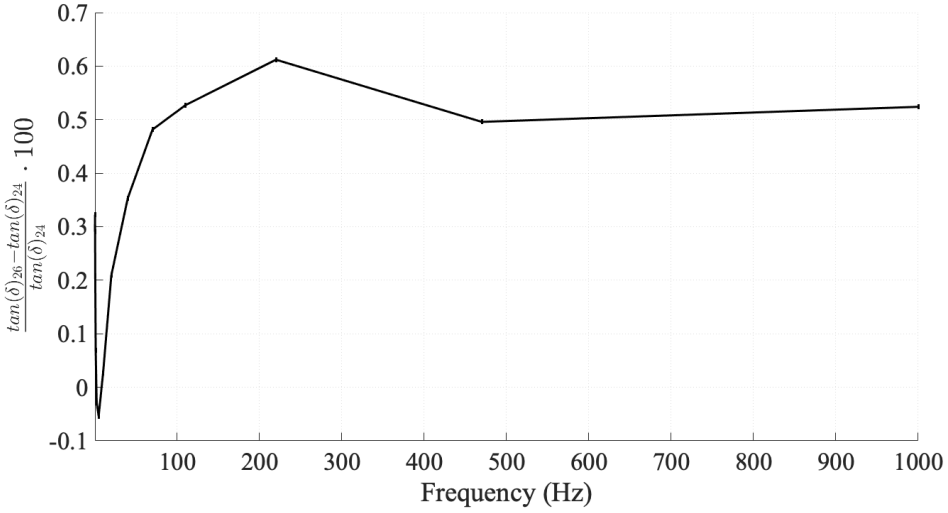

Figure 4.3: Relative difference between the loss factor measurement after 24 and 26 hours in percentage.

4.2 Bulk resistivity results and discussion

In this section, first, it will be explained how the data is processed. Then, the results will be presented and discussed. Finally, two aspects, measurements at high humidity and the measured current response will be analysed in depth.

The data obtained from the measurements performed on material 3 at 20% relative humidity, 30 °C are plotted in Figure 4.4. The 3 current measurements when a 1 kV voltage is applied are shown on the left side. The corresponding bulk resistivities, calculated using Equation 2.3, are shown on the right side.

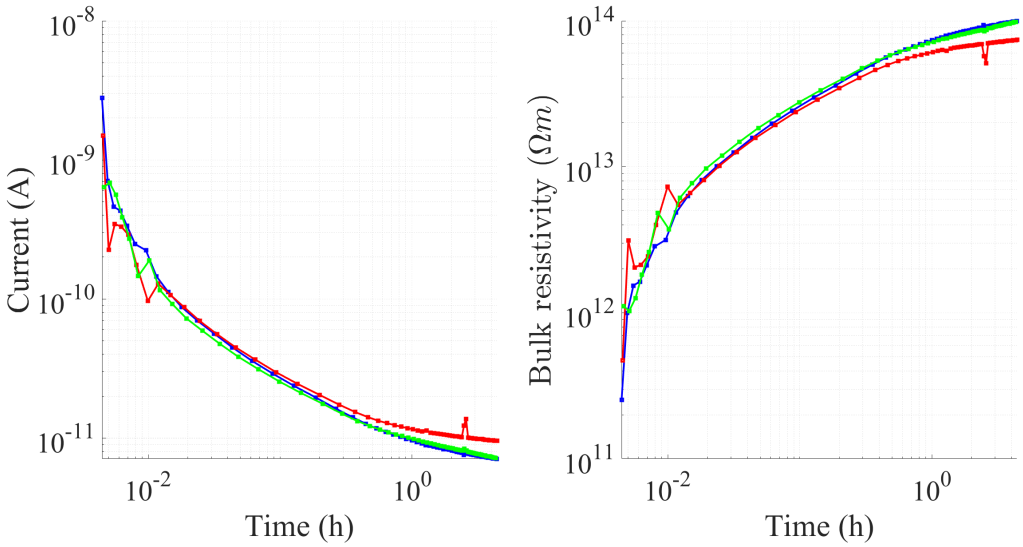

Figure 4.4: Material 3 at 20% relative humidity, 30 °C.

The average bulk resistivities during the last hour of measurement (ρ_i) are presented in Table 4.1.

Table 4.1: Average resistivities in the last hour of measurement for material 3 at 20% humidity, 30 °C.

Channel	1	2	3
ρ_i (Ωm)	$9.6038 \cdot 10^{13}$	$7.2293 \cdot 10^{13}$	$9.3993 \cdot 10^{13}$

The bulk resistivity of the material is calculated as

$$\rho = \frac{\rho_1 + \rho_2 + \rho_3}{3} = 8.7441 \cdot 10^{13}\ \Omega m \tag{4.1}$$

and the standard deviation is calculated as

$$\sigma = \sqrt{\left(\frac{1}{3}\left[(\rho_1 - \rho)^2 + (\rho_2 - \rho)^2 + (\rho_3 - \rho)^2\right]\right)} = 1.0744 \cdot 10^{13}\ \Omega m \tag{4.2}$$

In Table 4.2 the obtained bulk resistivities for each material at each different ambient condition are presented. In Table 4.3 the standard deviations of the bulk resistivities for each material at each different ambient condition are presented.

For 60% relative humidity 60 °C and 90 % relative humidity the presented results correspond to the case in which the top electrodes are covered with Teflon tape as explained in section 3.3.2. Additionally, in the case of material 5 and Teflon at 90% humidity 30 °C, plastic bags are used to cover the top electrodes with the intention of trying to avoid a possible bridging of electrode 2 and guard along the surface of the Teflon tape between the connectors. This is shown in Figure 4.5. No significant differences are observed in the results though.

Figure 4.5: Plastic bag to protect the electrodes from water condensation.

Resistivities are studied for 3 variables, type of material, temperature and humidity. The obtained bulk resistivities are plotted below,

Table 4.2: Bulk resistivity results.

	Volume resistivity (Ωm)					
	20 % RH	30 % RH	60 % RH		90 % RH	
	30 °C	60 °C	30 °C	60 °C	30 °C	60 °C
Material 3	$8.74 \cdot 10^{13}$	$5.05 \cdot 10^{12}$	$8.17 \cdot 10^{12}$	$8.79 \cdot 10^{11}$	$1.09 \cdot 10^{12}$	$7.14 \cdot 10^{11}$
Material 4	$3.43 \cdot 10^{13}$	$2.55 \cdot 10^{12}$	$4.83 \cdot 10^{12}$	$5.63 \cdot 10^{11}$	$2.12 \cdot 10^{12}$	$3.36 \cdot 10^{11}$
Material 5	$1.64 \cdot 10^{13}$	$1.82 \cdot 10^{12}$	$2.82 \cdot 10^{12}$	$3.44 \cdot 10^{11}$	$1.06 \cdot 10^{12}$	$9.60 \cdot 10^{10}$
Teflon	$4.03 \cdot 10^{15}$	-	-	-	$8.35 \cdot 10^{11}$	-

Table 4.3: Bulk resistivity standard deviations.

	Volume resistivity standard deviation (Ωm)					
	20 % RH	30 % RH	60 % RH		90 % RH	
	30 °C	60 °C	30 °C	60 °C	30 °C	60 °C
Material 3	$1.07 \cdot 10^{13}$ (12.29 %)	$5.36 \cdot 10^{11}$ (10.63 %)	$4.04 \cdot 10^{12}$ (49.40 %)	$2.58 \cdot 10^{11}$ (29.36 %)	$6.87 \cdot 10^{11}$ (62.98 %)	$1.39 \cdot 10^{11}$ (19.43 %)
Material 4	$1.24 \cdot 10^{12}$ (3.60 %)	$3.49 \cdot 10^{11}$ (13.67 %)	$1.90 \cdot 10^{12}$ (39.30 %)	$9.64 \cdot 10^{10}$ (17.12 %)	$9.73 \cdot 10^{11}$ (45.87 %)	$3.04 \cdot 10^{10}$ (9.08%)
Material 5	$5.21 \cdot 10^{12}$ (31.66 %)	$9.92 \cdot 10^{10}$ (5.46 %)	$1.12 \cdot 10^{12}$ (39.69 %)	$1.09 \cdot 10^{11}$ (31.69 %)	$1.61 \cdot 10^{11}$ (15.17 %)	$2.61 \cdot 10^{10}$ (27.25 %)
Teflon	$1.41 \cdot 10^{15}$ (35.02 %)	-	-	-	$3.08 \cdot 10^{11}$ (36.90 %)	-

keeping each time one variable constant so that results can be easily interpreted and trends can be established.

In Figures 4.6 and 4.7 the different SiR resistivities are plotted for 30 and 60 °C respectively. It can be observed that the resistivities are lower for higher humidities. Comparing the different material resistivities, material 4 has a lower resistivity than material 3 and material 5 has a lower resistivity than material 4. This trend is only broken in material 3 for the highest humidity level at 30 °C.

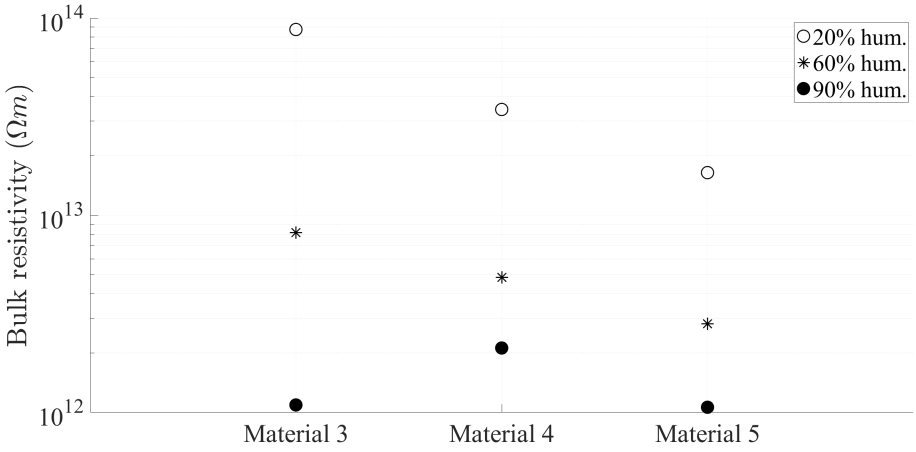

Figure 4.6: Bulk resistivities at 30 °C.

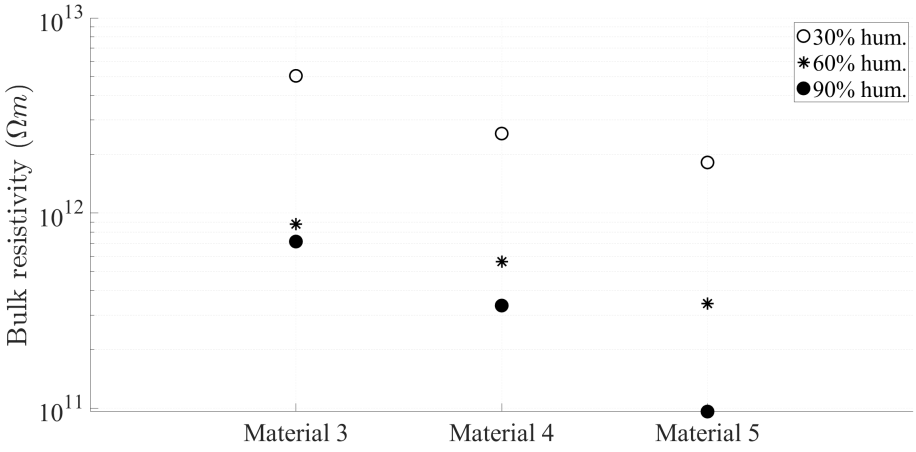

Figure 4.7: Bulk resistivities at 60 °C.

In Figures 4.8 to 4.10 the different SiR resistivities are plotted for low, medium and high humidity. In addition to the previously identified trends it is observed that for a higher temperature, resistivity reduces.

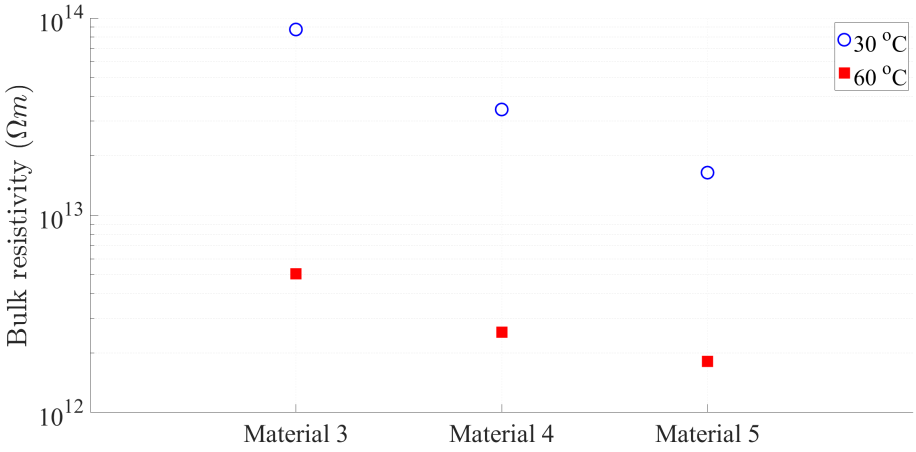

Figure 4.8: Bulk resistivities at 20-30% humidity.

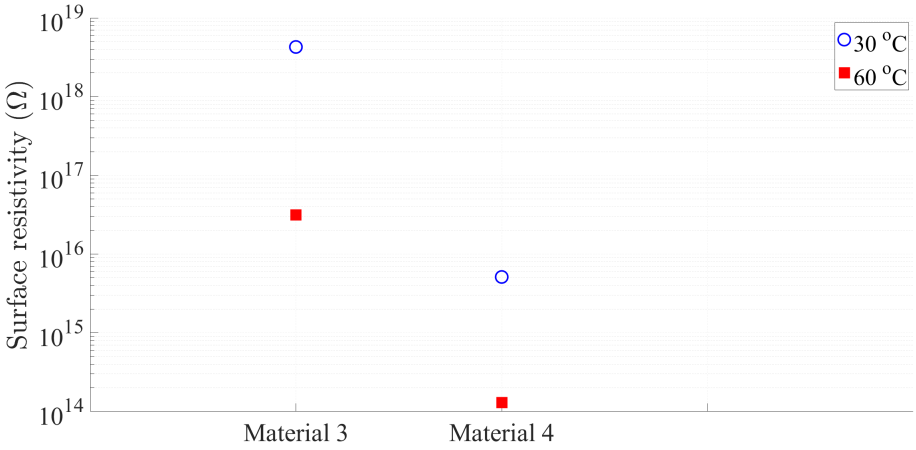

Figure 4.9: Bulk resistivities at 60% humidity.

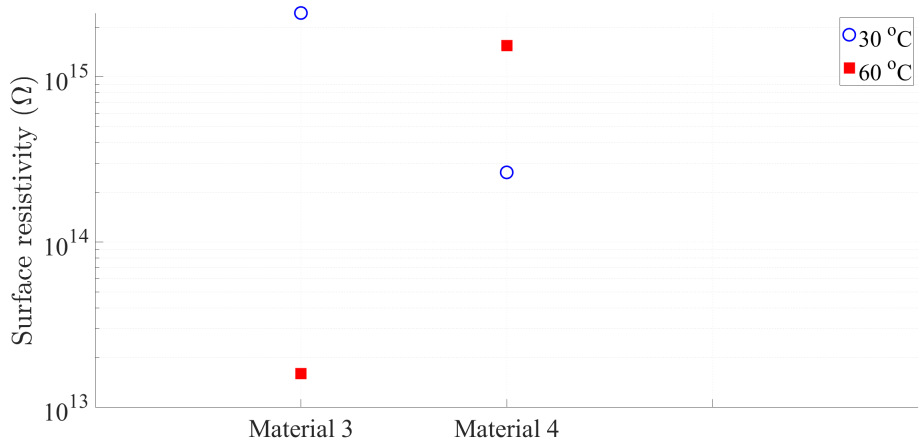

Figure 4.10: Bulk resistivities at 90% humidity.

In Figures 4.11 to 4.14 the bulk resistivities for each material are plotted. In the case of Teflon, a big variation in bulk resistivity is observed for a change in relative humidity. Such a big variation was not expected since Teflon is a less porous material than SiR. One of the possible reasons behind this behaviour is the inadequacy of the brass electrodes to perform resistivity measurements with Teflon. Teflon is a rigid material and thus the contact with the brass electrode may not be good. This could be solved by using a conductive rubber layer between the brass electrode and Teflon.

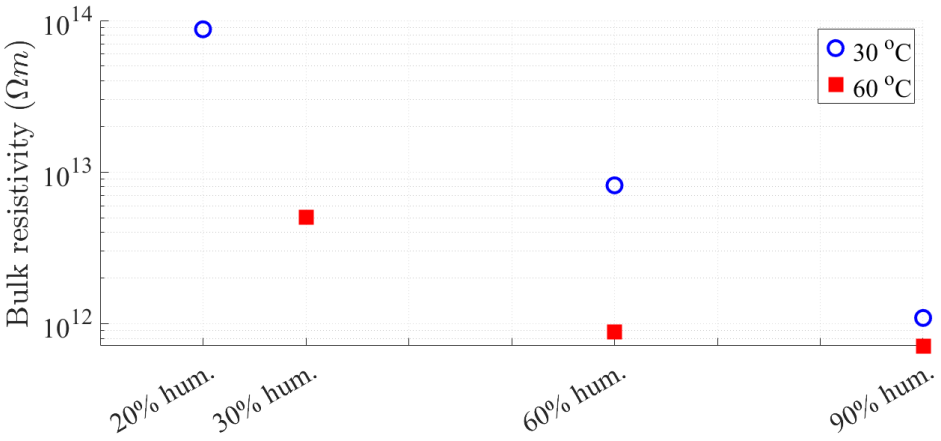

Figure 4.11: Bulk resistivities of material 3 under different temperature and humidity conditions.

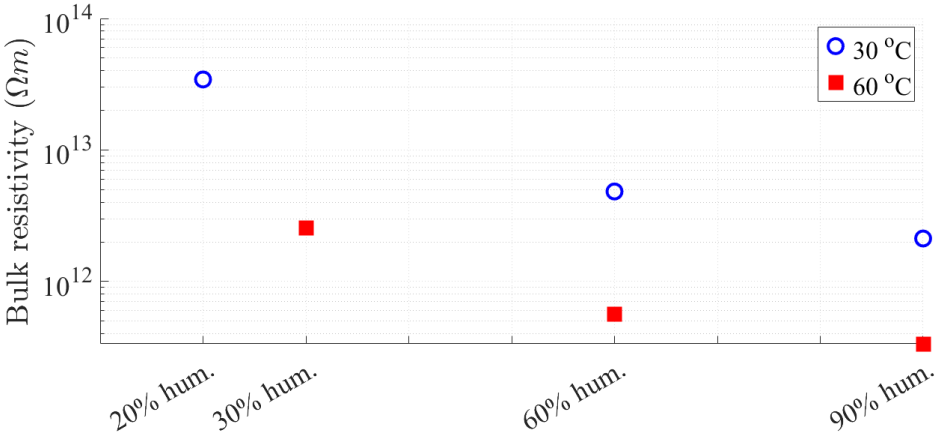

Figure 4.12: Bulk resistivities of material 4 under different temperature and humidity conditions.

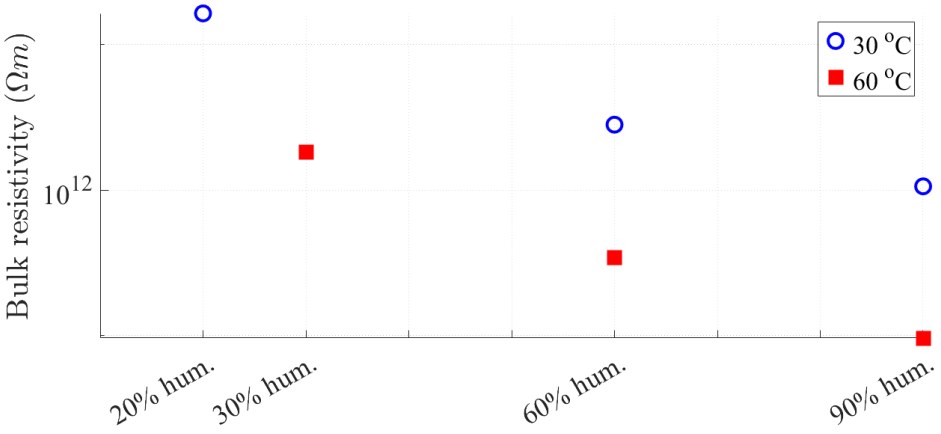

Figure 4.13: Bulk resistivities of material 5 under different temperature and humidity conditions.

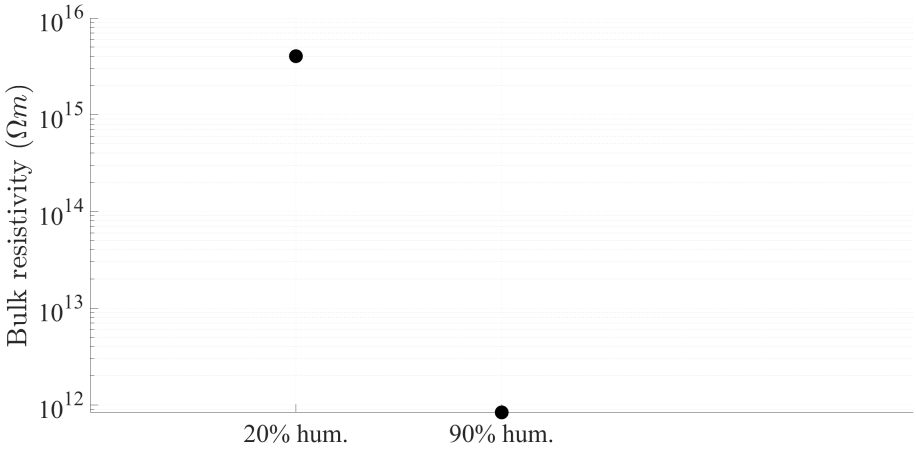

Figure 4.14: Bulk resistivities of Teflon.

4.2.1 High humidity results

As can be seen when comparing Figure 4.4 with Figures 4.15 to 4.17 current measurements become more noisy in high humidity conditions for all the measurement methods indicated in section 3.3.2. The noise appears earlier in the case of guard without Teflon tape. It is believed that this behaviour is caused by the discontinuous bridging of the electrodes due to water condensation.

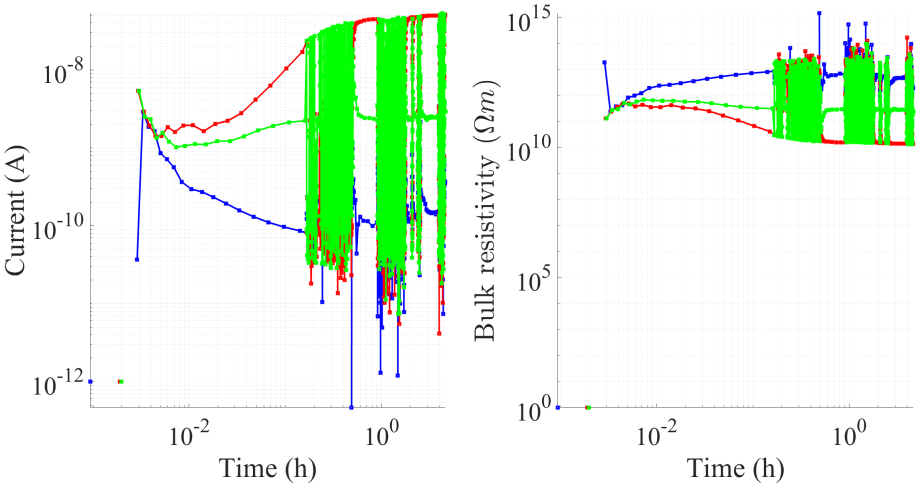

Figure 4.15: Material 3 current and bulk resistivity at 90% relative humidity 30 °C for a measurement with guard but not tape.

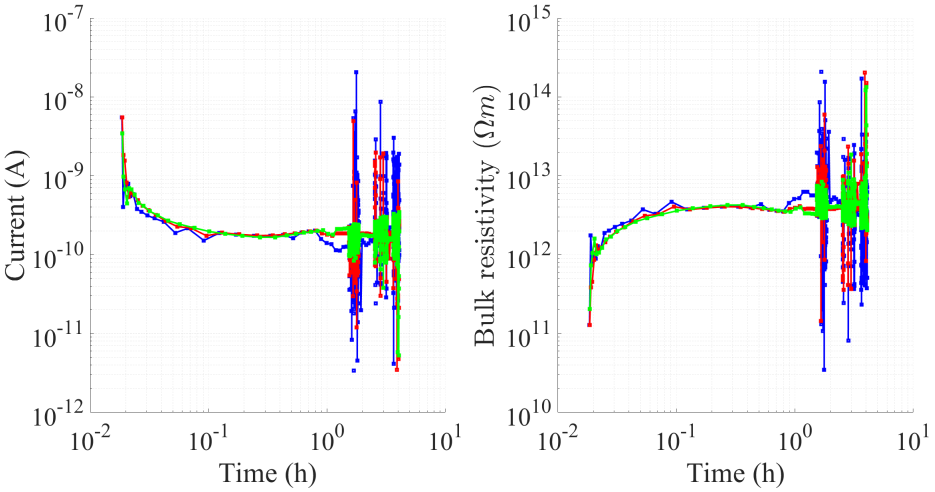

Figure 4.16: Material 3 current and bulk resistivity at 90% relative humidity 30 °C for a measurement with guard and Teflon tape.

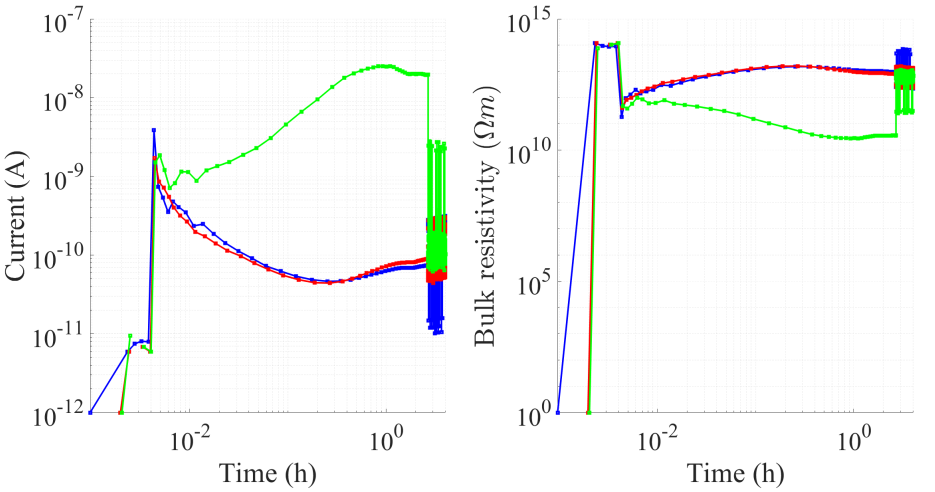

Figure 4.17: Material 3 current and bulk resistivity at 90% relative humidity 30 °C for a measurement without guard.

Tables 4.4 to 4.5 show the resistivity measured at 90% relative humidity 30 °C using the different measurement methods. The results are also plotted in Figure 4.18.

In the case of the resistivity measurement of material 5 with Teflon tape the electrodes were actually covered with plastic bags as shown in Figure 4.5.

It is observed that the resistivity values are in the same range for the 3 different methods. The trend of having lower resistivity in material

4 than 3 and in material 5 than 4 is only kept for the measurements without guard. Lower resistivity values were expected for the measurements without guard with respect to the rest. This is because of the higher expected current (current along the surface of the sample is not removed from the measurement). However this is not the case. This could indicate that there is a systematic bridging of the electrodes for all the tried methods.

The fact that similar values are obtained with Teflon tape and with plastic bags could indicate that the bridging of the electrodes happens due to the leakage of condensed water trough the bottom of the guard.

Table 4.4: Bulk resistivities at 90% relative humidity 30 °C using different procedures.

	Volume resistivity (Ωm)		
	Guard no tape	Guard with tape	No guard
Material 3	$3.16 \cdot 10^{11}$	$1.09 \cdot 10^{12}$	$5.95 \cdot 10^{12}$
Material 4	$8.29 \cdot 10^{11}$	$2.12 \cdot 10^{12}$	$1.39 \cdot 10^{12}$
Material 5	$1.75 \cdot 10^{12}$	$3.45 \cdot 10^{11}$	$1.06 \cdot 10^{12}$

Table 4.5: Bulk resistivities standard deviations at 90% relative humidity 30 °C using different procedures.

	Volume resistivity standard deviation (Ωm)		
	Guard no tape	Guard with tape	No guard
Material 3	$2.88 \cdot 10^{11}$ (91.20 %)	$6.87 \cdot 10^{11}$ (62.98 %)	$2.77 \cdot 10^{12}$ (46.53 %)
Material 4	$4.51 \cdot 10^{11}$ (54.33 %)	$9.73 \cdot 10^{11}$ (45.87 %)	$8.48 \cdot 10^{11}$ (60.95 %)
Material 5	$3.93 \cdot 10^{11}$ (22.53 %)	$1.61 \cdot 10^{11}$ (15.17 %)	$1.18 \cdot 10^{11}$ (34.14 %)

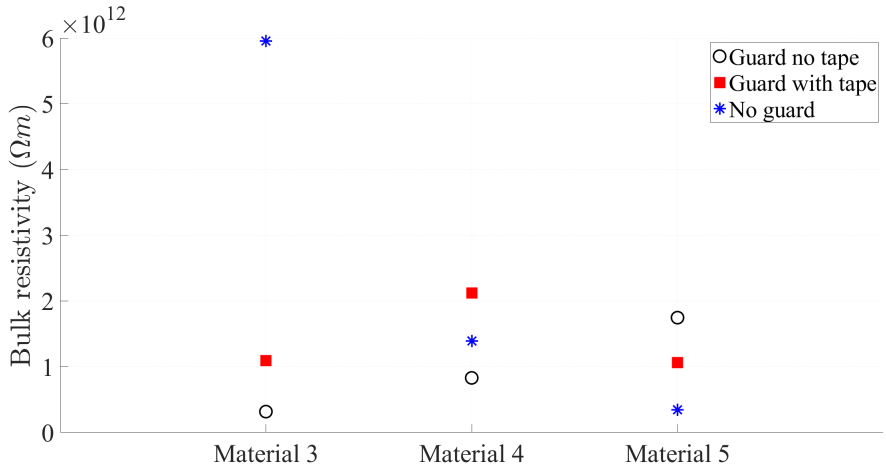

Figure 4.18: Bulk resistivities at 90% relative humidity 30 °C using different procedures.

4.2.2 Current response

Figure 4.19 shows the expected behaviour in the current, a decreasing exponential. However, when the temperature is increased, the current reaches a minimum an starts to increase as depicted in Figure 4.20. As humidity and temperature is further increased (see Figures 4.21 and 4.22) the current starts to go down again. An oscillating behaviour is confirmed by the 13 hour measurement on material 5 shown in Figure 4.23. It appears that for higher temperatures and humidities the oscillations happen earlier.

The presence of these oscillations means steady state has not yet been fully achieved after 4 hours.

In order to try to find an explanation for these oscillations in the current, one has to look into the charge dynamics in the dielectric material. Charges drift in the dielectric towards the electrode of opposite polarity where they accumulate and enhance the field in the electrode-dielectric interface. This boosts charge injection from electrode to dielectric material, current increases. Some of this charges drift towards the electrode of opposite polarity and some of them recombine with the opposite polarity charges. As a result the field reduces again in the electrode-dielectric material interface, injection reduces and current reduces. As charges of opposite polarity (heterocharges) start to accumulate again near the electrodes, the same cycle repeats.

The time it takes for the oscillations to appear and their period reduces with temperature and humidity because the conductivity of the material increases, making the charge dynamics faster.

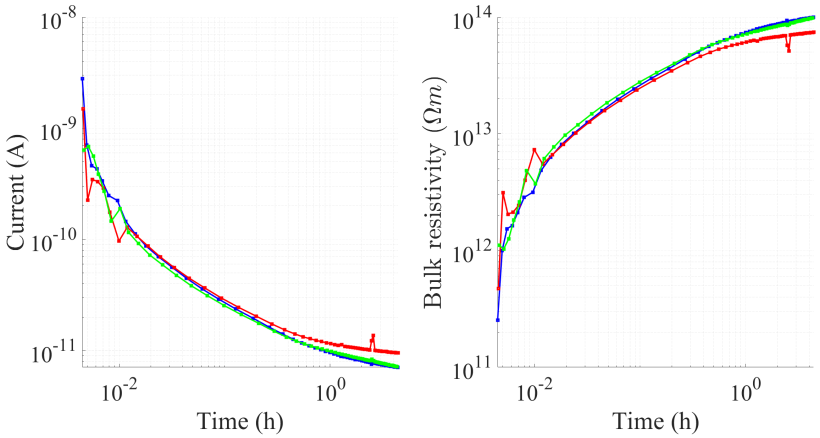

Figure 4.19: Material 3 at 20% relative humidity, 30 °C.

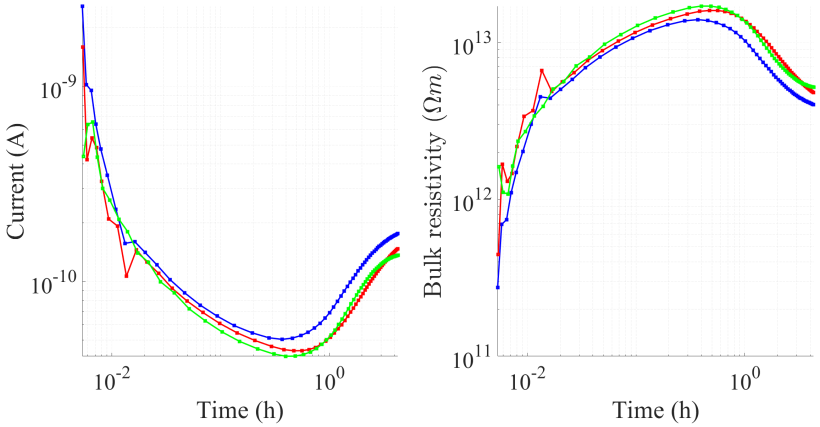

Figure 4.20: Material 3 at 20% relative humidity, 60 °C.

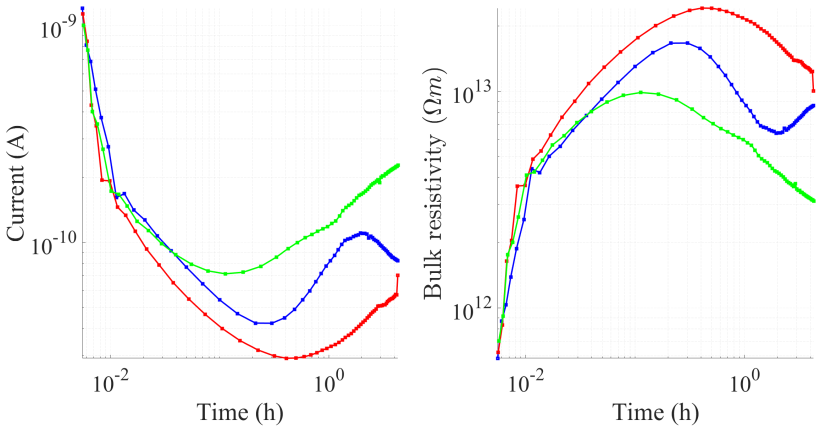

Figure 4.21: Material 3 at 60% relative humidity, 30 °C.

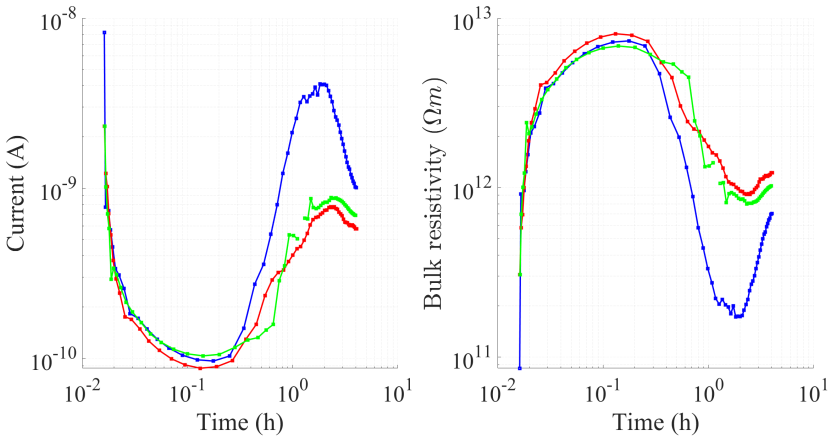

Figure 4.22: Material 3 at 60% relative humidity, 60 °C.

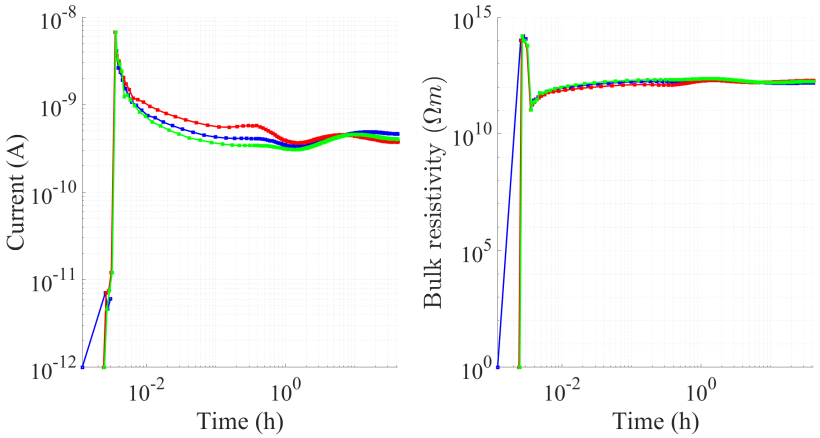

Figure 4.23: Material 5 at 20% relative humidity, 60 °C.

4.3 Surface resistivity results and discussion

In this section, first, it will be explained how the data is processed and then, the results will be presented and discussed. Finally, high humidity measurements will be analysed in depth.

Differently to bulk resistivity measurements, only one measurement is taken per material and temperature and humidity condition because of time limitations. The data obtained from one of the measurements is plotted in Figure 4.24. The current measurement when a 1 kV voltage is applied to material 4 at 30% relative humidity, 60 °C is shown on the left side. The corresponding calculated surface resistivity is shown on the right side.

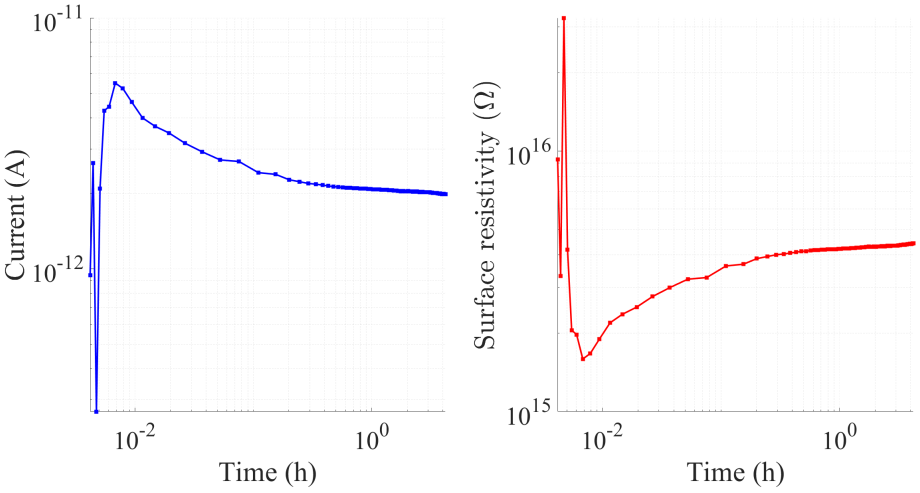

Figure 4.24: Material 4 at 30% relative humidity, 60 °C.

The surface resistivity values that are presented and discussed below are the average resistivities in the last hour of measurement.

In Table 4.6 the obtained surface resistivities for each material and each different ambient condition are presented. The noise level starts for currents below 10^{-13} A or, using Equation 2.9, for resistivities above $9 \cdot 10^{16}$. Measurements at noise level are shaded in grey in the table. Their values are uncertain.

Table 4.6: Surface resistivity results.

	Surface resistivity (Ω)					
	30 % RH		60 % RH		90 % RH	
	30 deg	60 deg	30 deg	60 deg	30 deg	60 deg
Material 3	$6.89 \cdot 10^{17}$	$1.47 \cdot 10^{17}$	$4.28 \cdot 10^{18}$	$3.13 \cdot 10^{16}$	$2.44 \cdot 10^{15}$	$1.61 \cdot 10^{13}$
Material 4	$6.74 \cdot 10^{16}$	$4.37 \cdot 10^{15}$	$5.13 \cdot 10^{15}$	$1.30 \cdot 10^{14}$	$2.64 \cdot 10^{14}$	$1.55 \cdot 10^{15}$
Teflon	$1.15 \cdot 10^{18}$	-	$1.18 \cdot 10^{18}$	-	$8.85 \cdot 10^{11}$	-

Resistivities are measured for 3 variables, type of material, temperature and humidity. The obtained surface resistivities are plotted below, keeping each time one variable constant so that results can be easily interpreted and trends can be established. Measurements at noise level are encircled in green.

In Figures 4.25 and 4.26 the different SiR resistivities are plotted for 30 °C and 60 °C respectively. As expected it is observed that at higher humidities the resistivity is lower. This is not the case, however, for a couple of points. Looking at Figure 4.25 and 4.30 it appears that the resistivity of material 3 at 30% relative humidity 30 °C should be higher than the resistivity of material 3 at 60% relative humidity 30 °C. Looking at Figure 4.26 and 4.31 it appears that the resistivity of material 4 at 90% relative humidity 60 °C should be lower than the resistivity of material 4 at 60% relative humidity 60 °C. The trend observed in bulk resistivity measurements that pointed at material 3 having a higher resistivity than material 4 is also observed in surface resistivity measurements except for the resistivity of material 4 at 90% relative humidity 60 °C.

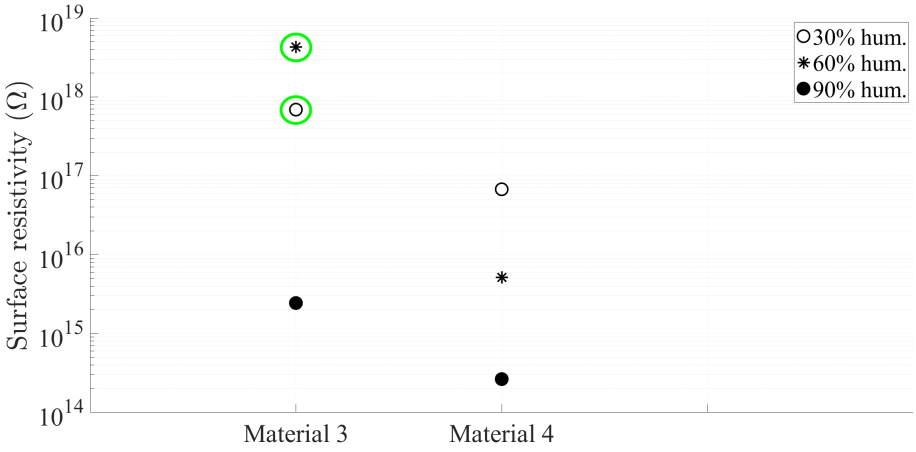

Figure 4.25: Surface resistivities at 30 °C.Measurements at noise level are encircled in green.

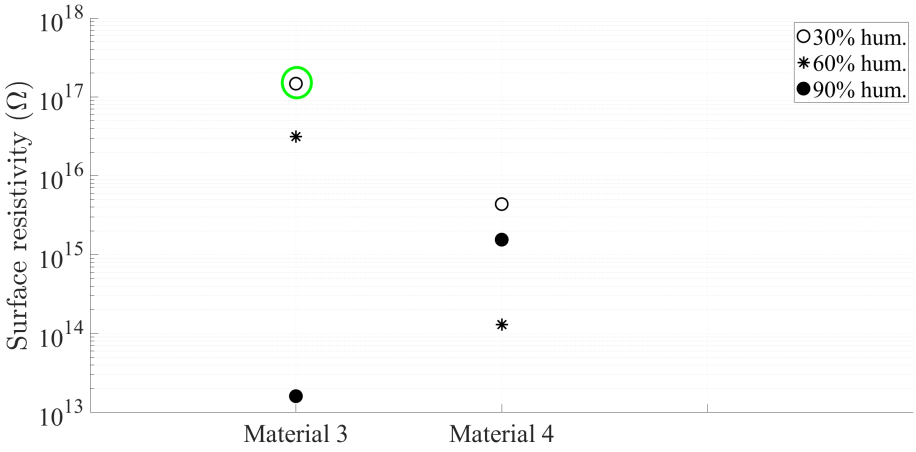

Figure 4.26: Surface resistivities at 60 °C. Measurements at noise level are encircled in green.

In Figures 4.27 to 4.29 the different SiR resistivities are plotted for low, medium and high humidity. It is observed that for higher temperatures the resistivity reduces.

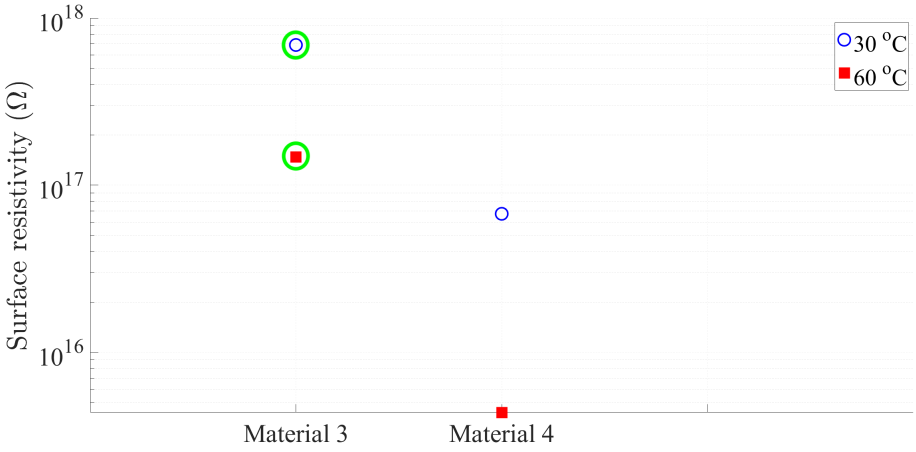

Figure 4.27: Surface resistivities at 30% humidity. Measurements at noise level are encircled in green.

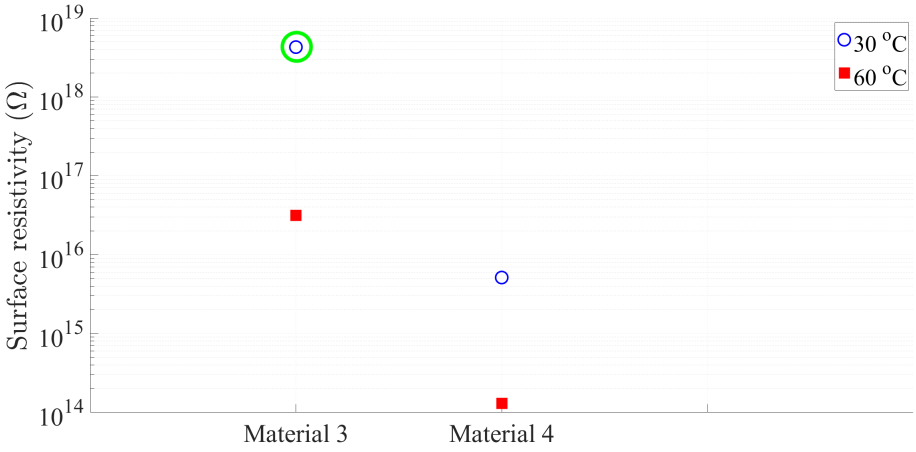

Figure 4.28: Surface resistivities at 60% humidity. Measurements at noise level are encircled in green.

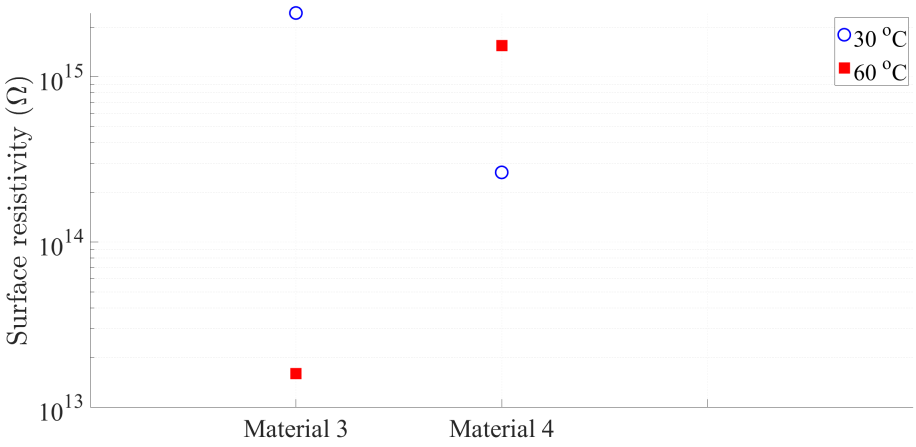

Figure 4.29: Surface resistivities at 90% humidity.

In figs. 4.30 to 4.32 the surface resistivities for each material are plotted.

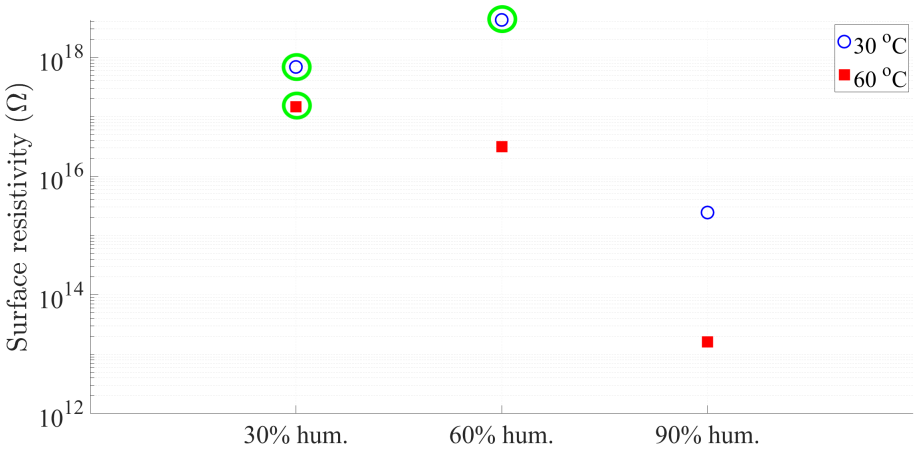

Figure 4.30: Surface resistivities of material 3 under different temperature and humidity conditions. Measurements at noise level are encircled in green.

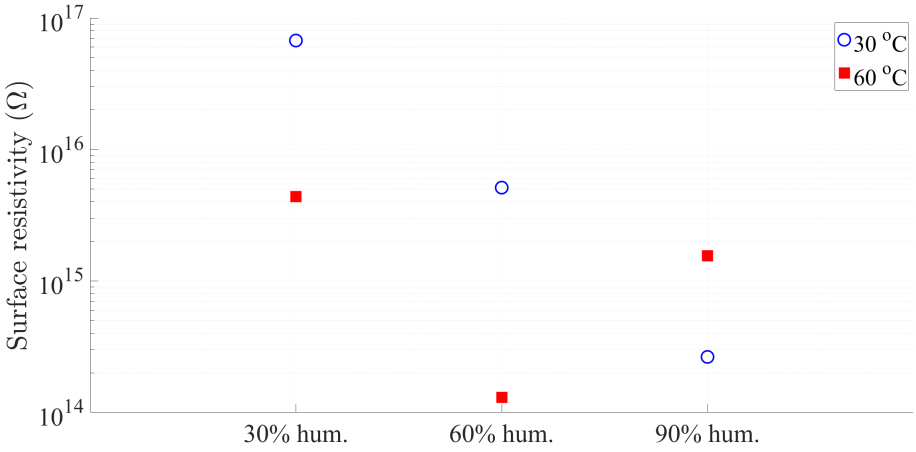

Figure 4.31: Surface resistivities of material 4 under different temperature and humidity conditions.

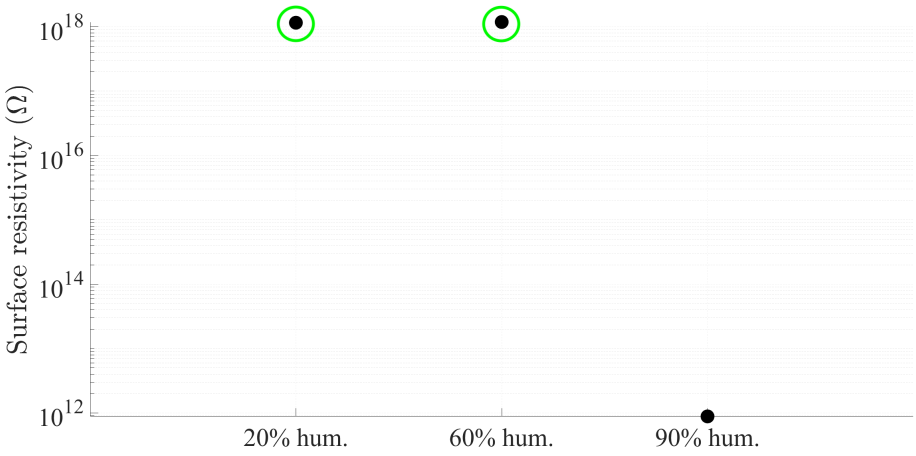

Figure 4.32: Surface resistivities of Teflon. Measurements at noise level are encircled in green.

4.3.1 High humidity results

It is observed both in material 3 and 4 that at 90% relative humidity 30 °C the current measurement becomes disperse during the first minutes. However, at 90% relative humidity 60 °C the measurement are again stable. The hypothesis is that for 90% relative humidity 30 °C water condensates into isolated water droplets. The electrodes are bridged when discharges between the different water droplets occur that lead to a path for the current. This leads to the behaviour observed in

Figure 4.33. At 90% relative humidity 60 °C however, the absolute humidity is higher leading to a greater condensation which causes the appearance of a continuous water layer on top of the samples. This water layer constitutes a path for the current that bridges the electrodes leading to the behaviour observed in Figure 4.34.

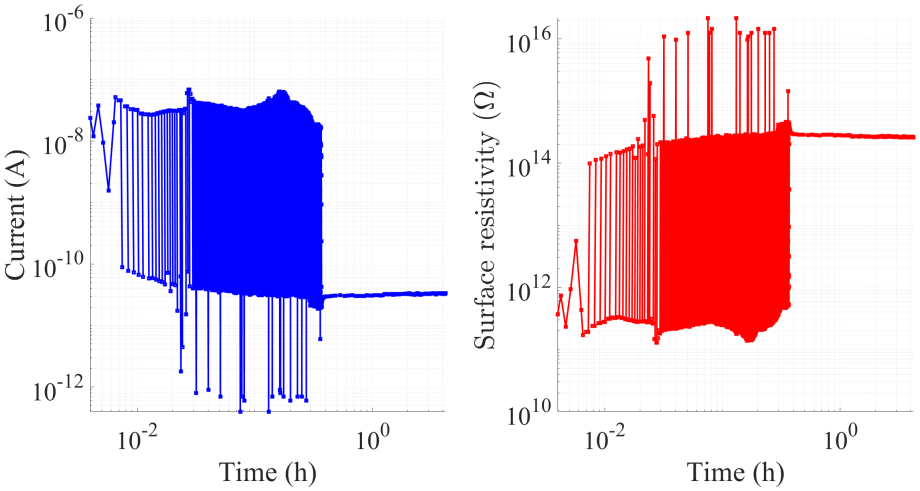

Figure 4.33: Material 4 at 90% relative humidity, 30 °C.

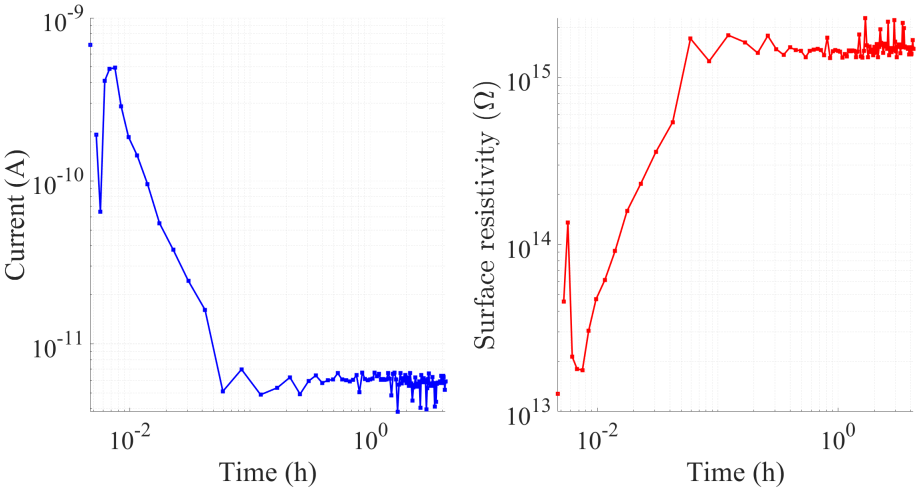

Figure 4.34: Material 4 at 90% relative humidity, 60 °C.

There is still to answer the question of why the current becomes smooth after approximately the first half hour in Figure 4.33. Here the hypothesis is that due to the application of an electric field, the hydrophobicity of the material reduces and a continuous water layer appears after some time.

Two SiR samples of material 3 were exposed to 90 % relative humidity 60 °C for more than 24 hours. A voltage of 1 kV was then applied to one of the samples using the surface resistivity measurement arrangement. Considering the distance between electrode 2 and ring electrode is 15 mm, the applied field was 0.0667 kV/mm. Hidrophobicity is studied using the spray method described in [12]. SiR samples are positioned horizontally. According to [12] the less percentage of the material surface is covered with water and the more circular the shape of the water droplets is, the higher the hydrophobicity of the material. As can be seen in Figure 4.35 it cannot be concluded from the test that the application of a voltage leads to a reduction in hydrophobicity.

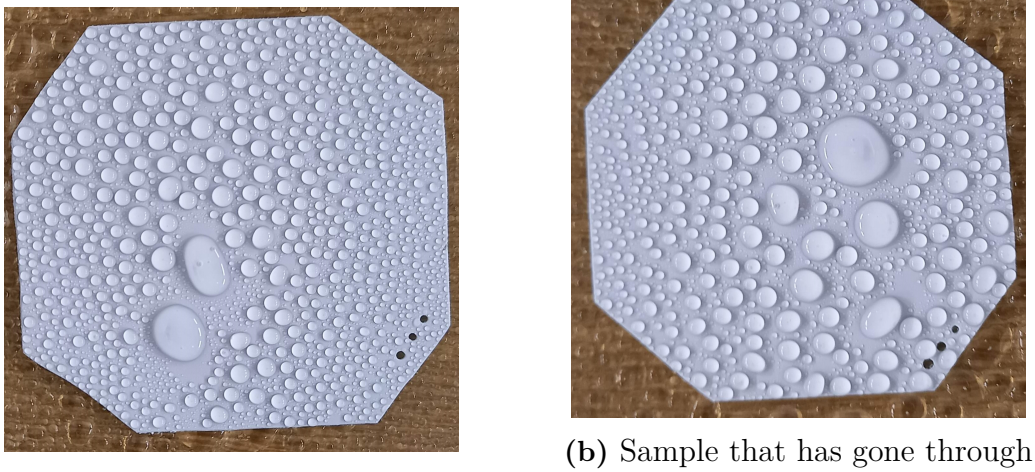

(a) Fresh sample. No voltage is applied.

(b) Sample that has gone through multiple measurements. 1 kV voltage is applied for 10 minutes after exposure.

Figure 4.35: Hydrophobicity test after conditioning the samples for more than 24 hours at 90% relative humidity 60 ^oC.

4.4 Sustainability aspects

The results obtained in this project will enable to make better predictions on how charges accumulate on the silicon rubber housing of different insulation systems in the presence of DC fields. As a result better estimations of the electric fields that the insulation systems have to withstand will be available. More reliable insulating systems will be manufactured and chosen for different projects. This increases the reliability of HVDC systems as a whole, making them more attractive. HVDC systems facilitate the integration of renewable energy

sources in the grid because, first, they enable the connection of distant offshore wind farms and second, they make the grid more resilient by connecting distant points and interconnecting asynchronous networks. Increasing the resiliency of the grid is key to be able to increase the penetration of renewable energy sources because they are intermittent in most cases.

5

Conclusions

It has been shown that an exposure time of 24 hours to the desired humidity conditions is enough for the bulk resistivity measurement of silicon rubber.

Bulk resistivity of SiR reduces with temperature and humidity. The bulk resistivity of material 3 is greater than the bulk resistivity of material 4 and the bulk resistivity of the latter is greater than the bulk resistivity of material 5. The bulk resistivity of Teflon reduces with humidity to a greater degree than SiR. This was not expected since Teflon is a less porous material than SiR. This raises doubts about the confidence in the results. Teflon is a rigid material and thus the contact with the brass electrodes is not good

In bulk resistivity measurements at high humidities water condensation is believed to cause bridging of measurement and guard electrodes. Several methods have been explored to avoid this but none of them has proven to be fully satisfactory.

Four hours is not enough time for the current to fully reach steady state. There are oscillations in the current that occur earlier for higher temperatures and humidities.

Surface resistivity of SiR reduces with temperature and humidity. The surface resistivity of material 3 is greater than the surface resistivity of material 4. A couple o measurements do not follow the expected trends.

Several surface resistivity measurements lie in the noise level.

At 90% relative humidity the results from the surface resistivity measurements suggest that there is a bridging of the electrodes through a condensed water layer on top of the sample.

The dependency of SiR surface resistivity with humidity and temperature is greater than the dependency of SiR bulk resistivity with humidity and temperature. It can be seen in the results that surface resistivity changes a maximum of 4 orders of magnitude with humidity while bulk resistivity changes a maximum of 2 orders of magnitude. Also, surface resistivity changes a maximum of 2 orders of magnitude with temperature while bulk resistivity changes a maximum of 1 order of magnitude.

Surface resistivity is more sensitive to humidity and temperature variations than bulk resistivity.

6

Future work

Salt solutions are a cheap method to obtain a steady state humidity level in a closed chamber, however, some inconveniences have been encountered. The achieved steady state humidity values have not always exactly matched. Setting the humidity to a certain value can be a slow process. It is recommended to use a humidity chamber in future work.

The method of measuring the evolution of the loss factor could be used to determine more precisely the minimum exposure time for the material under test.

Using conductive rubber in the Teflon-electrode interface is proposed.

In bulk resistivity measurements at high humidities it is proposed to explore and additional method to try and avoid the bridging of the electrodes. It is proposed to remove the guard from the electrode arrangement and use a big sample in order to minimise surface currents.

A longer measurement time than 4 hours is proposed so that a state closer to steady state is achieved.

Having to open the door of the oven to position the electrodes before performing bulk resistivity measurements leads to losing of the humidity conditions at the beginning of the measurement. Even though this is not expected to have a big effect on the measurements it would be better to have a measuring method where the oven did not have to be opened before performing the measurements. This could be achieved by having an automated system that positioned the electrodes on top of the samples. Alternatively, the determination of the bulk resistivity by measuring surface potential decay characteristics as described in [13] could be explored. This method also provides the advantage of keeping the top surface of the sample exposed to the ambient conditions during the measurement.

A greater number of surface resistivity measurements are needed in order to increase the certainty of the results.

It is proposed to raise the applied voltage in surface resistivity measurements for low temperatures and humidities in order to get currents above the noise level.

Bibliography

[1] A. Stan, S. Costinaș, and G. Ion, "Overview and assessment of HVDC current applications and future trends," *Energies*, vol. 15, 2 2022.

[2] State Grid Corporation of China, "Changji-Guquan ±1,100 kV UHV DC transmission project starts power transmission," 1 2019. [Online]. Available: https://web.archive.org/web/20200127003106/http://www.sgcc.com.cn/html/sgcc_main_en/col2017112406/2019-01/18/20190118183221870335071_1.shtml

[3] Hitachi Energy, "Product guide, composite station post insulators."

[4] D. Svensson, "Humidity dependence of charge accumulation on polymer-air interfaces for HVDC applications," Master's thesis, Chalmers University of Technology, Gothemburg, Sweden, 2021.

[5] L. Greenspan, "Humidity fixed points of binary saturated aqueous solutions," *Journal of Research of the National Bureau of Standards-A. Physics and Chemistry*, vol. 81.

[6] A. Rakowska and K. Hajdrowski, "Influence of different test conditions on volume resistivity of polymeric insulated cables and polyethylene samples," 2000.

[7] P. P. Tsai and R. R. Bresee, "Using field theory to measure surface resistivity of high-resistance polymeric films," *Journal of Applied Polymer Science*, vol. 82, pp. 2856–2862, 12 2001.

[8] S. Alam, "Surface potential dynamics on insulating polymers for HVDC applications," Ph.D. dissertation, Chalmers University of Technology, Gothemburg, Sweden, 2016.

[9] "Surface resistivity and surface resistance measurements using a concentric ring probe technique," 2003. [Online]. Available: https://www.researchgate.net/publication/237233852

[10] A. Küchler, *High Voltage Engineering: Fundamentals-Technology-Applications*. Springer, 2017.

[11] Y. A. Cengel, M. A. Boles, and M. Kanoğlu, *Thermodynamics: An Engineering Approach*, 9th ed. McGraw-hill New York, 2015.

[12] *Guidance on the measurement of hydrophobicity of insulator surfaces, IEC TS 62073*, International Electrotechnical Commission, 2016.

[13] S. Alam, Y. V. Serdyuk, and S. M. Gubanski, "Field-dependent electric conductivities of silicone rubbers deduced from measured currents and surface potential decay characteristics," *International Journal of Polymer Analysis and Characterization*, vol. 24, pp. 54–62, 1 2019.

DEPARTMENT OF ELECTRICAL ENGINEERING
CHALMERS UNIVERSITY OF TECHNOLOGY
Gothenburg, Sweden
www.chalmers.se

CHALMERS
UNIVERSITY OF TECHNOLOGY